Neural signatures of human fear conditioning: An updated and extended meta-analysis of fMRI studies

MA Fullana[1,2,3,12], BJ Harrison[4,12], C Soriano-Mas[5,6], B Vervliet[7], N Cardoner[3,8], A Àvila-Parcet[9] and J Radua[10,11]

[1]Anxiety Unit, Institute of Neuropsychiatry and Addictions, Hospital del Mar, CIBERSAM, Barcelona, Spain; [2]IMIM (Hospital del Mar Medical Research Institute), Barcelona, Spain;[3]Department of Psychiatry, Autonomous University of Barcelona, Barcelona, Spain; [4]Melbourne Neuropsychiatry Centre, Department of Psychiatry, The University of Melbourne,Melbourne, Victoria, Australia; [5]Department of Psychiatry, Bellvitge University Hospital-IDIBELL, CIBERSAM, Barcelona, Spain; [6]Department of Psychobiology and Methodology of Health Sciences, Autonomous University of Barcelona, Barcelona, Spain; [7]Center for Excellence on Generalization in Health and Psychopathology, University of KU Leuven, Leuven, Belgium; [8]Depression and Anxiety Unit, Mental Health Department, Parc Taulí Sabadell University Hospital, Barcelona, Spain; [9]Autonomous University of Barcelona, Barcelona, Spain; [10]Department of Psychosis Studies, Institute of Psychiatry, Psychology and Neuroscience, King's College London, London, UK and [11]Department of TranslationalNeuroimaging, FIDMAG Germanes Hospitalàries-CIBERSAM, Sant Boi de Llobregat, Barcelona, Spain.

Correspondence: Dr MA Fullana, Anxiety Unit, Institute of Neuropsychiatry and Addictions, Hospital del Mar, Passeig Marítim, 25-29, Barcelona 08003, Spain or Dr BJ Harrison, Melbourne Neuropsychiatry Centre, Department of Psychiatry, University of Melbourne, Office 345, Level 3, 161 Barry Street, Melbourne, Australia.

E-mail: miguelangelfullana@gmail.com or habj@unimelb.edu.au

[12]These authors equally contributed to this work.

ABSTRACT

Classical Pavlovian fear conditioning remains the most widely employed experimental model of fear and anxiety and continues to inform contemporary pathophysiological accounts of clinical anxiety disorders. Despite its widespread application in human and animal studies, the neurobiological basis of fear conditioning remains only partially understood. Here, we provide a comprehensive meta-analysis of human fear conditioning studies carried out with functional magnetic resonance imaging (fMRI) - yielding a pooled sample of 677 participants from 27 independent studies. As a distinguishing feature of this meta-analysis, original statistical brain maps were obtained from the authors of 13 of these studies. Our primary analyses demonstrate that human fear conditioning is associated with a consistent and robust pattern of neural activation across a hypothesized genuine network of brain regions resembling existing anatomical descriptions of the "central autonomic-interoceptive network". This finding is discussed with a particular emphasis on the neural substrates of conscious fear processing. Our associated meta-analysis of functional deactivations – a scarcely addressed dynamic in fMRI fear conditioning studies – also suggests the existence of a coordinated brain response potentially underlying "safety signal" (i.e., non-threat) processing. We attempt to provide an integrated summary on these findings with the view that they may inform ongoing studies of fear conditioning processes both in healthy and clinical populations, as investigated with neuroimaging and other experimental approaches.

Introduction

Learning to identify and to respond to signals of threat is highly adaptive and critical to survival, however when this process becomes dysregulated, in the form of aberrant fear responses to innocuous events, full-blown anxiety disorders can emerge.[1] Numerous experimental studies have focused on elucidating the precise mechanisms of adaptive and maladaptive fear learning processes in animals and humans across behavioral, experiential and neural domains. To do so, the vast majority of studies have employed classical Pavlovian fear conditioning (henceforth "fear conditioning"), a simple and powerful method to model fear learning in the laboratory. In this procedure, an initially neutral stimulus comes to elicit a fear response after being paired with an aversive stimulus (unconditioned stimulus, US). This paired association transforms the neural stimulus into a conditioned stimulus (CS) with the capacity to elicit anticipatory fear responses. Fear conditioning has become widely regarded as a valid experimental model of clinical anxiety disorders, and thus it is hoped that further advances in the scientific study of fear conditioning processes will yield translational benefits in the form of optimized pathophysiological models of these common mental health disorders.[2]

Several experimental paradigms have been developed for the study of fear conditioning. Most typically, these paradigms focus on establishing conditioned fear responses (conditioned response, CR) to a specific foreground cue (*cue-conditioning*) or a general background context (*context conditioning*). They may include variations in the number of CSs presented (*single-cue*, when one CS is presented vs. *differential conditioning*, when two or more CSs are presented) or in the temporal relationship between the CS and US (*delay conditioning*, when the US is presented at the end of the CS vs. *trace conditioning*, when a gap occurs between CS offset and US onset).

These paradigms have now been extensively applied, particularly with regard to investigations of the neurobiological substrates of fear/anxiety processes. One important example comes from human functional magnetic resonance imaging (fMRI) studies, which have sought to clarify the role of specific brain regions and associated networks in fear conditioning processes, particularly delay differential cue-conditioning. In an effort to summarize the results of such studies and to reach a genuine consensus regarding the common neural substrate of human differential fear conditioning, two existing meta-analyses have been reported. Initially, Etkin and Wager[3] analyzed 10 studies published between 1998 and 2005, which included a total of 117 healthy participants. Their results indicated that fear conditioning, overall, is characterized by consistent neural activation of an extended "fear network" including the dorsal anterior cingulate cortex (dACC), bilateral anterior insular cortex (AIC), amygdala, orbitofrontal cortex, anterior thalamus, ventral putamen and pallidum, and midbrain substantia nigra/ventral tegmentum. One limitation of this meta-analysis was that it included both "instructed" and "uninstructed" studies. In the former situation, participants are told that a particular CS will be followed by a US (i.e., they are "contingency aware") and therefore the CR during the CS-US conditioning trials relates to the expression of an already learned association. In the uninstructed studies, participants are initially unable to predict when the US will occur; that is, the CS-US conditioning trials capture the learning process itself.

In addressing this limitation, Mechias *et al*.[4] conducted separate meta-analyses of instructed (n=10; 162 participants) and uninstructed (n=15; 198 participants) fear conditioning studies published between 1998 and 2008. Across both study types, some commonality was observed, particularly with regard to the consistent involvement of the rostral dACC and AIC. However, meta-analytic results for the uninstructed

conditioning studies were noted as less robust - or more inconsistent. Limitations of this second meta-analysis include the fact that it combined results from a trace (as opposed to delay) conditioning study,[5] which has been shown to evoke distinct neural correlates.[6] In addition, almost half of the included studies involved participants performing a concurrent cognitive task during fear conditioning. This dual-task feature is an important caveat since previous laboratory-based studies have shown that cognitive demands may have a significant impact on fear conditioning processes.[7] Finally, both of these former meta-analyses only considered neural activations (i.e., relative activity increases) occurring in response to conditioned vs. non-conditioned stimuli (CS+ > CS-), as opposed to considering both activations and *deactivations* corresponding to this experimental contrast (i.e., relative activity decreases, CS+ < CS). As is now broadly recognized in the neuroimaging field, functional deactivations may be as equally informative for understanding the neural substrates of complex mental activities,[8-10] including emotion processing.[8, 11, 12]

To address some of the limitations of these past meta-analyses and to provide an updated characterization of the neural signatures of human fear conditioning as studied with fMRI, we have implemented Anisotropic Effect-Size Signed Differential Mapping (AES-SDM).[13] AES-SDM is a novel neuroimaging meta-analytic approach that is capable of combining tabulated brain activation/deactivation results (i.e., regional peak statistic and coordinate information) with actual empirical voxel-wise "brain maps" of activations and deactivations (e.g., statistical parametric maps; SPMs). We concentrated on uninstructed fear conditioning studies because (contrary to instructed studies, which primarily capture fear *expression*), they focus on fear *learning,* which has a stronger theoretical link with the hypothesized etiology and pathophysiology of clinical anxiety disorders.[14] In doing so, we were able to compile

whole-brain imaging results from 27 independent fMRI studies involving 677 healthy adult participants. As an additional and novel distinguishing feature of this analysis, original SPMs were obtained from the corresponding authors of 13 of these 27 studies. Including original SPMs, as opposed to including only peak regional effects (typically reported in tables of statistics), substantially increases the analyses statistical power[13] and may avoid reporting biases that are likely to affect certain brain regions, especially smaller subcortical regions that are poorly represented in commonly used stereotaxic atlases of the human brain.[15, 16] Furthermore, inclusion of this number of SPMs allowed, for the first time, the estimation of the task-specific optimal parameters for processing the peak information of the remaining studies.

To account for the moderating influence of several methodological and sociodemographic factors that may be highly likely to influence the results of fMRI fear conditioning studies,[17] we also performed several supplementary analyses. Of note, we purposefully investigated the influence of potential US confounding (i.e., CS-US co-presentation) on both activation and deactivation patterns and also investigated "early" vs. "late" conditioning phase effects, which have been reported to better capture the involvement of specific regions of interest, including greater involvement of the amygdala during early conditioning.[18] In conducting this meta-analysis, our primary goal was therefore to provide an updated and extended characterization of the neural signature of human fear conditioning as studied with fMRI.

Methods

Literature search and study selection

A comprehensive literature search using PubMed, Web of Knowledge and Scopus was

conducted of English-language peer-reviewed fMRI studies on cued fear conditioning in human healthy adults (age >18 years) published between January 1998 and November 2013. The search terms were: "fMRI" or "magnetic resonance imaging", "fear", "conditioning", "Pavlovian", and their combinations. Additionally, manual searches were conducted within review articles and via the reference lists of individual studies. Researchers in the area were also contacted with regard to potential unpublished data. If any studies contained participant group overlap, only the first reported study was included. If not originally reported, the corresponding authors of the identified studies were asked to provide additional details and whole-brain results where necessary and possible.

We focused on studies using a delay differential cue-conditioning paradigm given that other paradigms (e.g., trace or single-cue) appear to engage non-overlapping neural responses.[6, 19] We only included studies with an independent validation of successful fear response generation (e.g., via skin conductance recordings) and that conducted direct statistical comparisons between a CS+ and a CS- during conditioning. For pharmacological challenge/intervention studies, only placebo or control groups were included.

Studies were excluded if they either used masked CSs; USs with ambiguous meaning; employed changing CS-US contingencies; presented the US before conditioning; or combining context and cue conditioning in the same experiment. Dual-task studies employing attentional distraction features were also excluded, but studies where the dual task feature was intended to enhance/maintain vigilance were included (**Table 1**). We also excluded studies from which peak information or SPMs could not be retrieved, that did not report whole-brain statistical results, and/or whereby statistical thresholds varied across the assessment of different brain regions.

Studies with less than 10 participants were also excluded (see[20]).

We obtained original empirical SPMs of the primary contrasts of interest (CS+> CS-; CS+<CS-) for 13 datasets. For the remaining 14 studies, peak regional coordinate statistics were extracted and coded from the original paper or from supplementary data provided by corresponding authors (**Table 1S**). In certain studies, this contrast was based only on CSs+ *not* paired with the US (there was no US confounding) whereas others used "all" CS+ trials, and thus neural responses may be confounded by US-induced activity changes.[17] Additionally, in certain studies, all CSs trials during conditioning were included in the analysis, whereas in others "early" and "late" phases were compared. When more than one contrast was available for a dataset, we selected the contrast relating to the analysis of all trials. If this was not available, we focused on the "early" contrast, given that activation in some regions appears to be more pronounced during early conditioning phases.[17] However, based on available studies, we were able to conduct an "early" vs. "late" comparison to reconcile such findings.

The literature search, decisions on inclusion, and data extraction were all performed independently by two of the authors. For each dataset, several demographic and task-related variables were extracted (**Table 1**).

---Table 1 ----

Meta-analytic approach

Functional activation differences between the CS+ and the CS- were meta-analyzed using AES-SDM software, version 4.13 (www.sdmproject.com).[13, 21] This method, which has been validated and used in several structural and functional fMRI studies creates a brain map of the effect size of the difference between the two conditions

(CS+ and CS-) for each study (either from SPMs or from peak information), and afterwards conducts a voxelwise random-effects meta-analysis (weighting the studies for sample size and variance)[13, 20-22] (see **Supplementary Material**). In the present analysis, and for the first time, we were able to empirically derive the optimal parameters (40% anisotropy and kernel FWHM=20mm) for creating the effect size maps of the studies from which peak information but not SPMs were available. [10]

To assess the robustness of findings, we conducted a jackknife sensitivity analysis. [20] We also repeated the analysis after including only those studies considering both activations and deactivations (n=19), or only those studies for which SPMs were available (n=13). Finally, the I^2 index and Egger's method were used to assess for heterogeneity of effect sizes and publication bias respectively (see **Supplementary Material**).

We conducted an additional meta-analysis comparing studies with potential US confounding (n=11) to those with no US confounding (n=10) (**Table 1**). To reduce variability, we did not include studies with dual task features (n=6). As introduced above, a meta-analysis was also conducted of studies comparing "early" and "late" conditioning phase effects. Although an "early vs. late" contrast was only directly available from three studies, it could be estimated from the early and late contrast results of four additional studies taking into account the correlation between the early and late phases (estimated from the initial three studies). Despite only including seven studies, SPMs of four of them were available for this meta-analysis.

The potential influence of the following variables on estimated activations and deactivations was further explored by means of meta-regression: gender (% females); mean age of participants; presence of a pre-conditioning (habituation) phase; number

of CSs during conditioning; reinforcement rate; average CS-US delay; type of US (electric shock vs. other); and use of cognitive task.

Statistical significance was assessed with AES-SDM default thresholds (voxel-level $p < 0.005$ uncorrected, minimum extent 10 contiguous voxels), as previous simulations indicate that this threshold provides an optimal balance between sensitivity and false positive rate. [13] A more conservative threshold ($p < 0.0005$) was applied to meta-regression analyses in order to correct for the application of multiple tests. [23-25] For the sake of completeness, cluster-based corrected p-values are provided in all tables of results. [26] Results are reported in MNI space.

Results

Study characteristics

The final sample (**Figure 1S**) consisted of 27 independent datasets reporting a CS+ > CS- contrast (of which 19 also presented a CS+ < CS- contrast) including a total of 677 subjects (54% males), with a mean age of 25.37 years (Range: 20-36; SD=4.19). See **Table 1**.

Primary meta-analytic results

Seven large bilateral regional clusters were mapped as demonstrating consistently significant functional activations during differential fear conditioning (CS+ > CS). The major regions comprising these clusters were: 1) the anterior insular cortex (AIC) extending to the frontal operculum; 2) the ventral striatum (including ventral rostral

putamen, ventral pallidum, ventral caudate/nucleus accumbens; and approximate ventral tegmental area); and major thalamic nuclei (mediodorsal; centromedial, ventrolateral nuclei)- the latter referenced against thalamic nuclei probability maps from the SPM Anatomy Toolbox; 3) a large expanse of medial wall cortex including the pre-supplementary and supplementary motor areas and the dACC (both rostral and caudal divisions) and a distinct cluster of the dorsal-anterior precuneus; 4) second somatosensory cortex (SII) / parietal operculum; 5) dorsolateral prefrontal cortex (dlPFC; more prominently left-sided); 6) lateral premotor cortex; 7) ventral-posterior precuneus; and 8) lateral cerebellum. We also note the relevant involvement of smaller subcortical regions including the septal-hypothalamic zone and midbrain/dorsal pons, which contains the periaqueductal grey, parabrachial nucleus, reticular formation, raphe nuclei (pontine, midbrain) and locus coeruleus. An additional cluster was also mapped to the pontomedullary junction (**Figure 1**; **Table 2S**).

---Figure 1 ---

Nine large bilateral regional clusters were also mapped as demonstrating consistently significant deactivations during differential fear conditioning (CS+<CS-). These deactivation clusters comprised: 1) lateral and midline primary somatosensory (SI) cortex as well as the dorsal posterior insular cortex; 2) dorsal anterior prefrontal cortex; 3) ventromedial prefrontal cortex (vmPFC); 4) posterior cingulate cortex, including retrosplenial cortex, hippocampus, and lateral inferior and middle temporal cortex; 5) lateral orbitofrontal cortex; 6) inferior parietal cortex (complete angular gyrus extending to intraparietal sulcus); 7) lateral retrosplenial cortex; 8) posterior cerebellum; 9) dorsal caudate nucleus (body); and 10) dorsal-posterior precuneus (**Figure 2; Table 2S**).

---Figure 2 ---

Figure 2S displays the activation/deactivation results together across 24 axial slices of a whole-brain anatomical reference volume. Our corresponding robustness analyses indicated that all results were highly replicable and that there was neither substantial heterogeneity, nor evidence of potential publication bias in the main results (**Supplementary Material**).

Additional meta-analyses

A direct comparison of studies with potential US confounding versus those without such confounding indicated a greater involvement of the rostral dACC/dmPFC, bilateral ventral AIC, ventral striatum (ventral-mid caudate and approximate ventral tegmental area) and right SII in the latter scenario (**Figure 3**); versus a greater relative involvement of anterior calcarine sulcus in studies with potential confounding. Comparison of the two study types also indicated greater relative deactivation of the bilateral intraparietal sulcus, vmPFC and left hippocampus in studies without potential confounding (see **Table 3S**). However, it must be noted that studies with potential confounding also had, on average, a higher reinforcement rate (85%) compared to those without those without potential confounding (50%). (See expanded discussion in **Supplementary Material**).

---Figure 3 ---

The "early vs. late" meta-analysis indicated that the early phase was associated with greater relative activation of the medial thalamus, left SII, and left AIC (**Figure 3S**, **Table 4S**). By comparison, the late phase was associated with greater activation of

the subgenual ACC/vmPFC extending to medial orbitofrontal cortex and the right anterior hippocampus, as well as greater deactivation of the right precuneus.

Meta-regression analyses

Gender had no influence on the primary activation results. Younger age was associated with significantly greater activation of the right AIC extending to frontal operculum, right dlPFC, pre-SMA, and the left frontal operculum as well as greater deactivation of the left anterior hippocampus and posterior fusiform gyrus **(Table 5S)**.

The results of the meta-regression with respect to task-specific features are summarized in **Figure 4** (see also **Table 5S).** The use of a pre-conditioning phase significantly reduced conditioning-related activation of several regions. Of these regions, all but the ventral ACC (**Figure 4a**) overlapped with regions implicated in the primary meta-analysis (**Figure 1**). By comparison, activation of the left anterior hippocampus was greater with the use of a pre-conditioning phase (**Figure 4b**).

Presenting a higher number of CS trials during conditioning was associated with greater activation of the left ventral caudate nucleus extending to the nucleus accumbens (**Figure 4c**). A higher CS-US reinforcement rate reduced strength of activation of the rostral dACC/dmPFC (**Figure 4d**), right parietal operculum (SII) and a small cluster of right AIC. A longer delay between the CS-US was associated with greater activation of the subgenual ACC and vmPFC and less activation of the right parietal operculum/SII, pre-SMA and right premotor cortex (**Figure 4e**). The use of a tactile electric shock US (compared to other US types) was associated with greater activation of the left caudal dorsal ACC/ventral SMA (**Figure 4f**). Finally, the concurrent use of cognitive tasks reduced the activation of the bilateral mid AIC.

---Figure 4 ---

Discussion

This updated and extended meta-analysis has identified a highly consistent pattern of functional brain activation and deactivation associated with human differential fear conditioning. Robustness analyses confirmed the strength of the primary findings, while supplementary analyses were able to address the influence of specific task features on the associated patterns of brain activity.

Functional activations: An integrated perspective

The notion that human differential fear conditioning, as studied with fMRI, activates a consistent distributed set of brain regions, or extended "fear network",[17, 27, 28] was wholly confirmed by the current meta-analysis. Whilst only a small number of the same studies were included in our meta-analysis compared to the aforementioned analyses (**Table 6S**),[3, 4] striking overlap emerged in the specific pattern of brain activation observed. We therefore conclude that in spite of the considerable methodological diversity that exists across individual fear conditioning studies, these studies consistently evoke a common large-scale brain activation response. [17]

With the goal of providing an integrated perspective, we hypothesize that this common pattern of activation is genuinely consistent with the engagement of a large-scale brain functional network; that is, a coordinated pattern of brain activation across anatomically distributed brain regions with well-known anatomical connectivity. In this context, we emphasize in particular the involvement of medial wall

"cingulofrontal cortex" regions, including the dorsal anterior cingulate cortex (dACC), together with the bilateral anterior insular cortex (AIC).

Considerable evidence now supports the view that these brain regions form major cortical components of a large-scale brain network with specialized functional relevance to homeostatic autonomic and behavioral (including affective) regulation.[29-32] More specifically, this brain network has been linked to *interoception* – the sense of the physiological condition of the entire body – including the representation of higher-order interoceptive feelings in terms of subjective emotional awareness.[30] Within the framework of this "central autonomic-interoceptive network", the AIC and dACC are conceptualized as the cortical major input-output components, whereby the AIC is responsible for generating an integrated awareness of one's cognitive, affective, and physical state that becomes re-represented in the dACC in order to facilitate homeostatic autonomic and behavioral responses.[30, 33] Supporting this network perspective, co-activation of these brain regions has been routinely observed in human fMRI studies, either accompanying or directly (i.e., temporally) correlated with changes in physiological autonomic arousal measures.[30, 31, 33, 34] Relevantly, we also identified robust involvement of key subcortical viscerosensory (and visceromotor) processing sites, including the dorsal midbrain (PAG, PBN), ventromedial thalamus and hypothalamus,[30, 31, 33, 34] as well as the pontomedullary junction, which contains the nucleus of the solitary tract (NTS) – a principal convergence site for viscerosensory afferent relay to higher areas.[31] It therefore seems reasonable to suggest human fMRI fear conditioning studies primarily evoke a central autonomic-interoceptive network response that, in addition to representing autonomic responses to threat, also likely represent broader threat appraisal and response processes that cut across cognitive, motivational and psychomotor domains.

From the specific analysis of potential US confounding, we observed significantly greater activation of the rostral dACC/dmPFC, the ventral AIC, ventral striatum and SII when no such confounding existed. Hence, for these regions, it can be more confidently interpreted that their accompanying response to the CS+ was purely anticipatory in nature and unrelated to the generation of defensive autonomic responses to the US. Relevant overlap can also be noted between this analysis and the analysis of reinforcement rate, whereby higher reinforcement was associated with *reduced* activation of the same rostral dACC/dmPFC, right SII and ventral AIC regions (**Figure 4S**). Because those studies without potential confounding had generally lower reinforcement rates, these brain responses are likely represent the common influence of uncertainty or unpredictability, that is, where lower reinforcement rates increase uncertainty or unpredictability. Greater involvement of the rostral dACC/dmPFC is particularly interesting in view of recent work implicating this region specifically in the conscious appraisal of threat, with particular relevance to the subjective experience of fear and anxiety.[35] From these studies, there is evidence that a certain component of the rostral dACC/dmPFC response during fear conditioning is specifically cognitively modulated and dissociable from autonomic arousal changes.[35] By comparison, other components of the extended dACC/medial wall response are likely to represent the direct interaction between autonomic and cognitive states.[36, 37] The AIC has also been proposed to mediate higher-level appraisal and anticipatory processes with relevance to the conscious experience of fear and anxiety,[38] although this proposal has yet to be conclusively demonstrated beyond the more general hypothesized link between AIC function and interoceptive awareness. In summary, fMRI fear conditioning tasks evoke a primary neural signature that is anatomically consistent with the engagement of the central autonomic-interoceptive

network. This finding, taken with other recent evidence, endorses an emerging view that the functional activity of this brain system may have direct relevance to the conscious experience of fear and anxiety, in addition to non-conscious aspects of fear processing, [39] a view which is compatible with current appraisal theories. [35]

Functional deactivations: Neural correlate of "safety" signal processing?

Although derived from fewer studies, our analysis of functional deactivations also identified a robust and anatomically distributed pattern of activity change involving the ventromedial prefrontal cortex (vmPFC), lateral orbitofrontal cortex (OFC), hippocampus and posterior cingulate cortex (PCC). Deactivation of the vmPFC and PCC, in particular, has become recognized as a characteristic functional signature of the human "default mode network" (DMN) - a large-scale brain system that exhibits consistent functional decreases in activity in fMRI studies when conditions of goal-directed task performance are compared with conditions of low task demand, such as passive resting states.[8, 9] Thus, one possible interpretation of this deactivation effect is that responding to the CS- vs. CS+ corresponds with more "resting-like" DMN activity. While it is difficult to completely exclude this possibility, the following factors deserve some consideration. Firstly, processing of CS- is not a passive condition: it places specific demands on learning, attentional and cognitive evaluative processes.[40] Secondly, only partial involvement of DMN regions was observed in our meta-analysis– there was no characteristic deactivation of the extended dorsomedial PFC, which is commonly observed in fMRI studies.[41] Thirdly, non-DMN regions, including the lateral OFC and primary somatosensory cortex (SI) were also implicated as part of this robust deactivation pattern. Considered together, it seems more

reasonable to interpret this finding as representing a specific neural correlate of processing the CS- "safety" signal.

Previous fMRI studies of fear conditioning have argued that vmPFC deactivation is indeed likely to represent processing of the CS- as a non-threat or "safety" signal, with particular emphasis on fear response inhibition.[42, 43] Similar ideas have also been invoked in the context of fear extinction and fear reversal studies, where there is accumulating evidence to suggest that vmPFC activity may encode the distinction between non-threating and threating stimuli. Although the precise nature of vmPFC "safety" processing may vary across fear learning contexts, one possibility is that the distinction between CS- and CS+ signals evoke a common neural substrate for the dynamic representation of reward value, with CS- "safety" signals having an intrinsic positive reward value.[44] Co-deactivation of the lateral OFC is also interesting in this context, having been consistently implicated as part of the extended neural circuitry of reward associative learning, albeit with evidence existing for specialized contributions between medial and lateral vmPFC/OFC regions.[45]

Specific deactivation of the PCC/retrosplenial cortex together with the hippocampus is also interesting to consider with regards to the processing of the CS- as a "safety" signal. Both regions are well known components of an extended episodic memory network, and it has been proposed recently that the co-engagement of these areas may specifically encode episodic memory traces of the CS/US association. [46] Although hippocampal involvement has been more traditionally linked to trace conditioning and the declarative learning of discontinuous temporal associations, our findings raise the possibility that an episodic memory representation may be established during the specific processing of the CS-; potentially related to the establishment of contingency awareness (see [6]). Another possibility is that greater

PCC/hippocampal activation to the CS- represents a neural correlate of "relief" – related to the US omission (see [47]). Thus, although the specific meaning of functional deactivations in the context of fMRI fear conditioning studies remains speculative, the associated brain regions and the robustness of their response observed to the CS- versus CS+ -, as demonstrated via meta-analysis, should compel further investigations.

"Fear" vs. "threat conditioning"

It has been argued recently that the actual concept of "fear conditioning" be abandoned because it blurs the distinction between conscious and non-conscious fear processes.[48] In this sense, the term "fear" should be invoked only to define its conscious experience, whereas "threat conditioning" may be a preferable term when seeking to define the implicit (non-conscious) processes that control defense/survival responses elicited by threats. Although the boundary between these processes and their neuroanatomical representation remains a topic of debate, the idea of "fear" as primarily relating to consciously felt experience appears to resonate with the overall findings of fMRI conditioning studies, which consistently implicate a neural signature with direct hypothesized relevance to the conscious experience of emotions.[30, 31, 39]. This suggestion is not to imply that such studies only engage conscious fear processes, which would be an over-simplification, but that the prominent engagement of cortical regions, particularly the AIC and rostral dACC appears consistent with such notions.

Given the strong empirical link between amygdala circuitry and threat conditioning processes,[49] it is relevant that our meta-analysis did not characterize robust involvement of the amygdala region – as previously also highlighted in various independent studies[50, 51]. Other fMRI studies have reported transient amygdala

responses during early conditioning, [18] however this was neither apparent from our meta-analysis of early versus late acquisition phases. While the absence of amygdala involvement may be partly explained by technical constraints of fMRI and other reasons,[4, 17] it seems reasonable to also conclude that human fMRI fear conditioning experiments generally do not evoke consistent responses within the classical amygdala defense/threat detection circuitry.

Strengths and limitations

Strengths of the current analysis include the use of novel meta-analytic methods that combine the positive features of typical coordinate approaches with those from standard meta-analytic methods; the novel recreation of effect size maps using the optimal anisotropy and FWHM for the specific dataset; and the inclusion of 13 original SPMs to more effectively estimate the contrasts of interest.

Our study nevertheless has some limitations inherent to most meta-analyses: the different studies included employed various statistical thresholds, and although our methods provide excellent control for false positives, it is more difficult to avoid false negatives.[13] Additionally, the results of our meta-regression analyses were hampered by the low variability in some of the variables studied. Nevertheless, these analyses indicate that despite the robustness of the main findings, some demographic and experimental design features do have a tangible influence on the resulting neural signatures of fear conditioning (see expanded discussion in **Supplementary Material**). Also, default AES-SDM statistical thresholds are based on uncorrected p-values, because they are recommended for their optimal balance between sensitivity and false positive rate,[13] although we also reported cluster-based corrected p-values.

Lastly, the influence of some important factors related to fear conditioning, such as contingency awareness, could not be assessed because such data was rarely presented among the individual studies.

Conclusion

Classical Pavlovian fear conditioning will continue to inform our current understanding of fear and anxiety. The results of this meta-analysis suggest that when applied in the human neuroimaging context, these experiments may be especially useful for expanding knowledge of how fear and anxiety are experienced in subjective terms with a particular relevance to central interoceptive representations of brain-body interactions. It is notable that these relationships remain largely unexplored in the neuroscientific study of patients with clinical anxiety disorders, thus potentially representing a novel research avenue.

Supplementary information is available at Molecular Psychiatry's website

ACKNOWLEDGEMENTS

We thank the following authors for providing additional data or information not included in some original articles: M Andreatta, C Büchel, M Carter, H Critchley, J Dunsmoor, F Eippert, H Flor, J Hall, A Hermann, R Kalisch, J Kattoor, M Kindt, T Klucken, D Knight, TB Lonsdorf, M Menon, M Milad, C Merz, P Pauli, EA Phelps, L Romaniuk, D Schiller, D Schultz, V Spoormaker, R Stark, C Uhlmann, S van Well and R. Visser.

This work was supported by 'Miguel Servet' contracts from the Carlos III Health Institute (Spain) to CS-M (CP10/00604) and JR (CP14/00041), grants from Carlos III Health Institute/FEDER to MAF/NC (PI12/00273) and CS-M (PI13/01958), and an Australian NHMRC Project Grant to BJH (APP1025619).

CONFLICT OF INTEREST

The authors declare no conflict of interest.

References

1. Lissek S, Powers AS, McClure EB, Phelps EA, Woldehawariat G, Grillon C *et al.* Classical fear conditioning in the anxiety disorders: a meta-analysis. *Behav Res Ther* 2005; **43:** 1391-1424.
2. Kindt M. A behavioural neuroscience perspective on the aetiology and treatment of anxiety disorders. *Behav Res Ther* 2014; **62:** 24-36.
3. Etkin A, Wager TD. Functional neuroimaging of anxiety: a meta-analysis of emotional processing in PTSD, social anxiety disorder, and specific phobia. *Am J Psychiatry* 2007; **164:** 1476-1488.
4. Mechias ML, Etkin A, Kalisch R. A meta-analysis of instructed fear studies: implications for conscious appraisal of threat. *Neuroimage* 2010; **49:** 1760-1768.
5. Buchel C, Dolan RJ, Armony JL, Friston KJ. Amygdala-hippocampal involvement in human aversive trace conditioning revealed through event-related functional magnetic resonance imaging. *J Neurosci* 1999; **19:** 10869-10876.
6. Knight DC, Cheng DT, Smith CN, Stein EA, Helmstetter FJ. Neural substrates mediating human delay and trace fear conditioning. *J Neurosci* 2004; **24:** 218-228.
7. Carter RM, Hofstotter C, Tsuchiya N, Koch C. Working memory and fear conditioning. *Proc Natl Acad Sci U S A* 2003; **100:** 1399-1404.
8. Harrison BJ, Pujol J, Contreras-Rodriguez O, Soriano-Mas C, Lopez-Sola M, Deus J *et al.* Task-induced deactivation from rest extends beyond the default mode brain network. *PLoS One* 2011; **6:** e22964.

9. Harrison BJ, Pujol J, Lopez-Sola M, Hernandez-Ribas R, Deus J, Ortiz H *et al.* Consistency and functional specialization in the default mode brain network. *Proc Natl Acad Sci U S A* 2008; **105:** 9781-9786.

10. Radua J, Mataix-Cols D. Heterogeneity of coordinate-based meta-analyses of neuroimaging data: an example from studies in OCD – Authors' reply. *Br J Psychiatry* 2010; **197:** 77.

11. Radua J, Sarro S, Vigo T, Alonso-Lana S, Bonnin CM, Ortiz-Gil J *et al.* Common and specific brain responses to scenic emotional stimuli. *Brain Struct Funct* 2014; **219:** 1463-1472.

12. Ter Minassian A, Ricalens E, Humbert S, Duc F, Aube C, Beydon L. Dissociating anticipation from perception: Acute pain activates default mode network. *Hum Brain Mapp* 2013; **34:** 2228-2243.

13. Radua J, Mataix-Cols D, Phillips ML, El-Hage W, Kronhaus DM, Cardoner N *et al.* A new meta-analytic method for neuroimaging studies that combines reported peak coordinates and statistical parametric maps. *Eur Psychiatry* 2012; **27:** 605-611.

14. Mineka S, Zinbarg R. A contemporary learning theory perspective on the etiology of anxiety disorders: it's not what you thought it was. *Am Psychol* 2006; **61:** 10-26.

15. David SP, Ware JJ, Chu IM, Loftus PD, Fusar-Poli P, Radua J *et al.* Potential reporting bias in fMRI studies of the brain. *PLoS One* 2013; **8:** e70104.

16. Fusar-Poli P, Radua J, Frascarelli M, Mechelli A, Borgwardt S, Di Fabio F *et al.* Evidence of reporting biases in voxel-based morphometry (VBM) studies

of psychiatric and neurological disorders. *Hum Brain Mapp* 2014; **35:** 3052-3065.

17. Sehlmeyer C, Schoning S, Zwitserlood P, Pfleiderer B, Kircher T, Arolt V *et al.* Human fear conditioning and extinction in neuroimaging: a systematic review. *PLoS One* 2009; **4:** e5865.
18. LaBar KS, Gatenby JC, Gore JC, LeDoux JE, Phelps EA. Human amygdala activation during conditioned fear acquisition and extinction: a mixed-trial fMRI study. *Neuron* 1998; **20:** 937-945.
19. Cheng DT, Knight DC, Smith CN, Helmstetter FJ. Human amygdala activity during the expression of fear responses. *Behav Neurosci* 2006; **120:** 1187-1195.
20. Radua J, Mataix-Cols D. Voxel-wise meta-analysis of grey matter changes in obsessive-compulsive disorder. *Br J Psychiatry* 2009; **195:** 393-402.
21. Radua J, Rubia K, Canales-Rodriguez EJ, Pomarol-Clotet E, Fusar-Poli P, Mataix-Cols D. Anisotropic kernels for coordinate-based meta-analyses of neuroimaging studies. *Front Psychiatry* 2014; **5:** 13.
22. Radua J, van den Heuvel OA, Surguladze S, Mataix-Cols D. Meta-analytical comparison of voxel-based morphometry studies in obsessive-compulsive disorder vs other anxiety disorders. *Arch Gen Psychiatry* 2010; **67:** 701-711.
23. Hart H, Radua J, Mataix-Cols D, Rubia K. Meta-analysis of fMRI studies of timing in attention-deficit hyperactivity disorder (ADHD). *Neurosci Biobehav Rev* 2012; **36:** 2248-2256.
24. Lim L, Radua J, Rubia K. Gray matter abnormalities in childhood maltreatment: a voxel-wise meta-analysis. *Am J Psychiatry* 2014; **171:** 854-863.

25. Radua J, Borgwardt S, Crescini A, Mataix-Cols D, Meyer-Lindenberg A, McGuire PK *et al.* Multimodal meta-analysis of structural and functional brain changes in first episode psychosis and the effects of antipsychotic medication. *Neurosci Biobehav Rev* 2012; **36:** 2325-2333.

26. Friston KJ, Worsley KJ, Frackowiak RS, Mazziotta JC, Evans AC. Assessing the significance of focal activations using their spatial extent. *Hum Brain Mapp* 1994; **1:** 210-220.

27. Buchel C, Dolan RJ. Classical fear conditioning in functional neuroimaging. *Curr Opin Neurobiol* 2000; **10:** 219-223.

28. Kim JJ, Jung MW. Neural circuits and mechanisms involved in Pavlovian fear conditioning: a critical review. *Neurosci Biobehav Rev* 2006; **30:** 188-202.

29. Cameron OG. Visceral brain-body information transfer. *Neuroimage* 2009; **47:** 787-794.

30. Craig AD. How do you feel--now? The anterior insula and human awareness. *Nat Rev Neurosci* 2009; **10:** 59-70.

31. Critchley HD, Harrison NA. Visceral influences on brain and behavior. *Neuron* 2013; **77:** 624-638.

32. Saper CB. The central autonomic nervous system: conscious visceral perception and autonomic pattern generation. *Annu Rev Neurosci* 2002; **25:** 433-469.

33. Medford N, Critchley HD. Conjoint activity of anterior insular and anterior cingulate cortex: awareness and response. *Brain Struct Funct* 2010; **214:** 535-549.

34. Beissner F, Meissner K, Bar KJ, Napadow V. The autonomic brain: an activation likelihood estimation meta-analysis for central processing of autonomic function. *J Neurosci* 2013; **33:** 10503-10511.

35. Kalisch R, Gerlicher AM. Making a mountain out of a molehill: on the role of the rostral dorsal anterior cingulate and dorsomedial prefrontal cortex in conscious threat appraisal, catastrophizing, and worrying. *Neurosci Biobehav Rev* 2014; **42:** 1-8.

36. Critchley HD, Mathias CJ, Dolan RJ. Neural activity in the human brain relating to uncertainty and arousal during anticipation. *Neuron* 2001; **29:** 537-545.

37. Wager TD, van Ast VA, Hughes BL, Davidson ML, Lindquist MA, Ochsner KN. Brain mediators of cardiovascular responses to social threat, part II: Prefrontal-subcortical pathways and relationship with anxiety. *Neuroimage* 2009; **47:** 836-851.

38. Paulus MP, Stein MB. An insular view of anxiety. *Biol Psychiatry* 2006; **60:** 383-387.

39. Adolphs R. The biology of fear. *Curr Biol* 2013; **23:** R79-93.

40. van Well S, Visser RM, Scholte HS, Kindt M. Neural substrates of individual differences in human fear learning: evidence from concurrent fMRI, fear-potentiated startle, and US-expectancy data. *Cogn Affect Behav Neurosci* 2012; **12:** 499-512.

41. Christoff K, Gordon AM, Smallwood J, Smith R, Schooler JW. Experience sampling during fMRI reveals default network and executive system contributions to mind wandering. *Proc Natl Acad Sci U S A* 2009; **106:** 8719-8724.

42. Milad MR, Wright CI, Orr SP, Pitman RK, Quirk GJ, Rauch SL. Recall of fear extinction in humans activates the ventromedial prefrontal cortex and hippocampus in concert. *Biol Psychiatry* 2007; **62:** 446-454.

43. Schiller D, Levy I, Niv Y, LeDoux JE, Phelps EA. From fear to safety and back: reversal of fear in the human brain. *J Neurosci* 2008; **28:** 11517-11525.

44. Schiller D, Delgado MR. Overlapping neural systems mediating extinction, reversal and regulation of fear. *Trends Cogn Sci* 2010; **14:** 268-276.

45. Grabenhorst F, Rolls ET. Value, pleasure and choice in the ventral prefrontal cortex. *Trends Cogn Sci* 2011; **15:** 56-67.

46. Holt DJ, Coombs G, Zeidan MA, Goff DC, Milad MR. Failure of neural responses to safety cues in schizophrenia. *Arch Gen Psychiatry* 2012; **69:** 893-903.

47. Leknes S, Lee M, Berna C, Andersson J, Tracey I. Relief as a reward: hedonic and neural responses to safety from pain. *PLoS One* 2011; **6:** e17870.

48. LeDoux JE. Coming to terms with fear. *Proc Natl Acad Sci U S A* 2014; **111:** 2871-2878.

49. LeDoux JE. Emotional memory: in search of systems and synapses. *Ann N Y Acad Sci* 1993; **702:** 149-157.

50. Öhman A. Human fear conditioning and the amygdala. In: Whalen PJ, Phelps EA (eds). *The human amygdala*. Guilford Press: New York, 2009.

51. Phelps EA, Delgado MR, Nearing KI, LeDoux JE. Extinction learning in humans: role of the amygdala and vmPFC. *Neuron* 2004; **43:** 897-905.

52. Andreatta M, Fendt M, Muhlberger A, Wieser MJ, Imobersteg S, Yarali A *et al.* Onset and offset of aversive events establish distinct memories requiring fear and reward networks. *Learn Mem* 2012; **19:** 518-526.

53. Dunsmoor JE, Prince SE, Murty VP, Kragel PA, LaBar KS. Neurobehavioral mechanisms of human fear generalization. *Neuroimage* 2011; **55:** 1878-1888.

54. Eippert F, Gamer M, Buchel C. Neurobiological mechanisms underlying the blocking effect in aversive learning. *J Neurosci* 2012; **32:** 13164-13176.

55. Haritha AT, Wood KH, Ver Hoef LW, Knight DC. Human trace fear conditioning: right-lateralized cortical activity supports trace-interval processes. *Cogn Affect Behav Neurosci* 2013; **13:** 225-237.

56. Harrison BJ, Fullana MA, Soriano-Mas C, Via E, Pujol J, Martinez-Zalacain I *et al. A neural mediator of human anxiety sensitivity*. Manuscript submitted for publication.

57. Hermann A, Kupper Y, Schmitz A, Walter B, Vaitl D, Hennig J *et al.* Functional gene polymorphisms in the serotonin system and traumatic life events modulate the neural basis of fear acquisition and extinction. *PLoS One* 2012; **7:** e44352.

58. Kalisch R, Holt B, Petrovic P, De Martino B, Kloppel S, Buchel C *et al.* The NMDA agonist D-cycloserine facilitates fear memory consolidation in humans. *Cereb Cortex* 2009; **19:** 187-196.

59. Kattoor J, Gizewski ER, Kotsis V, Benson S, Gramsch C, Theysohn N *et al.* Fear conditioning in an abdominal pain model: neural responses during associative learning and extinction in healthy subjects. *PLoS One* 2013; **8:** e51149.

60. Klucken T, Schweckendiek J, Koppe G, Merz CJ, Kagerer S, Walter B *et al.* Neural correlates of disgust- and fear-conditioned responses. *Neuroscience* 2012; **201:** 209-218.

61. Knight DC, Waters NS, Bandettini PA. Neural substrates of explicit and implicit fear memory. *Neuroimage* 2009; **45:** 208-214.

62. Maier S, Szalkowski A, Kamphausen S, Perlov E, Feige B, Blechert J *et al.* Clarifying the role of the rostral dmPFC/dACC in fear/anxiety: learning, appraisal or expression? *PLoS One* 2012; **7:** e50120.

63. Menon M, Jensen J, Vitcu I, Graff-Guerrero A, Crawley A, Smith MA *et al.* Temporal difference modeling of the blood-oxygen level dependent response during aversive conditioning in humans: effects of dopaminergic modulation. *Biol Psychiatry* 2007; **62:** 765-772.

64. Merz CJ, Wolf OT, Schweckendiek J, Klucken T, Vaitl D, Stark R. Stress differentially affects fear conditioning in men and women. *Psychoneuroendocrinology* 2013; **38:** 2529-2541.

65. Merz CJ, Hermann A, Stark R, Wolf OT. Cortisol modifies extinction learning of recently acquired fear in men. *Soc Cogn Affect Neurosci* 2014; **9:** 1426-1434.

66. Milad MR, Quirk GJ, Pitman RK, Orr SP, Fischl B, Rauch SL. A role for the human dorsal anterior cingulate cortex in fear expression. *Biol Psychiatry* 2007; **62:** 1191-1194.

67. Milad MR, Furtak SC, Greenberg JL, Keshaviah A, Im JJ, Falkenstein MJ *et al.* Deficits in conditioned fear extinction in obsessive-compulsive disorder and

neurobiological changes in the fear circuit. *JAMA Psychiatry* 2013; **70:** 608-618.

68. Romaniuk L, Honey GD, King JR, Whalley HC, McIntosh AM, Levita L *et al.* Midbrain activation during Pavlovian conditioning and delusional symptoms in schizophrenia. *Arch Gen Psychiatry* 2010; **67**(12)**:** 1246-1254.

69. Schultz DH, Balderston NL, Helmstetter FJ. Resting-state connectivity of the amygdala is altered following Pavlovian fear conditioning. *Front Hum Neurosci* 2012; **6:** 242.

70. Sehlmeyer C, Dannlowski U, Schoning S, Kugel H, Pyka M, Pfleiderer B *et al.* Neural correlates of trait anxiety in fear extinction. *Psychol Med* 2011; **41:** 789-798.

71. Spoormaker VI, Schroter MS, Andrade KC, Dresler M, Kiem SA, Goya-Maldonado R *et al.* Effects of rapid eye movement sleep deprivation on fear extinction recall and prediction error signaling. *Hum Brain Mapp* 2012; **33:** 2362-2376.

72. Stark R, Wolf OT, Tabbert K, Kagerer S, Zimmermann M, Kirsch P *et al.* Influence of the stress hormone cortisol on fear conditioning in humans: evidence for sex differences in the response of the prefrontal cortex. *Neuroimage* 2006; **32:** 1290-1298.

73. Tabbert K, Stark R, Kirsch P, Vaitl D. Hemodynamic responses of the amygdala, the orbitofrontal cortex and the visual cortex during a fear conditioning paradigm. *Int J Psychophysiol* 2005; **57:** 15-23.

74. Visser RM, Scholte HS, Kindt M. Associative learning increases trial-by-trial similarity of BOLD-MRI patterns. *J Neurosci* 2011; **31**(33)**:** 12021-12028.

75. Visser RM, Scholte HS, Beemsterboer T, Kindt M. Neural pattern similarity predicts long-term fear memory. *Nat Neurosci* 2013; **16:** 388-390.

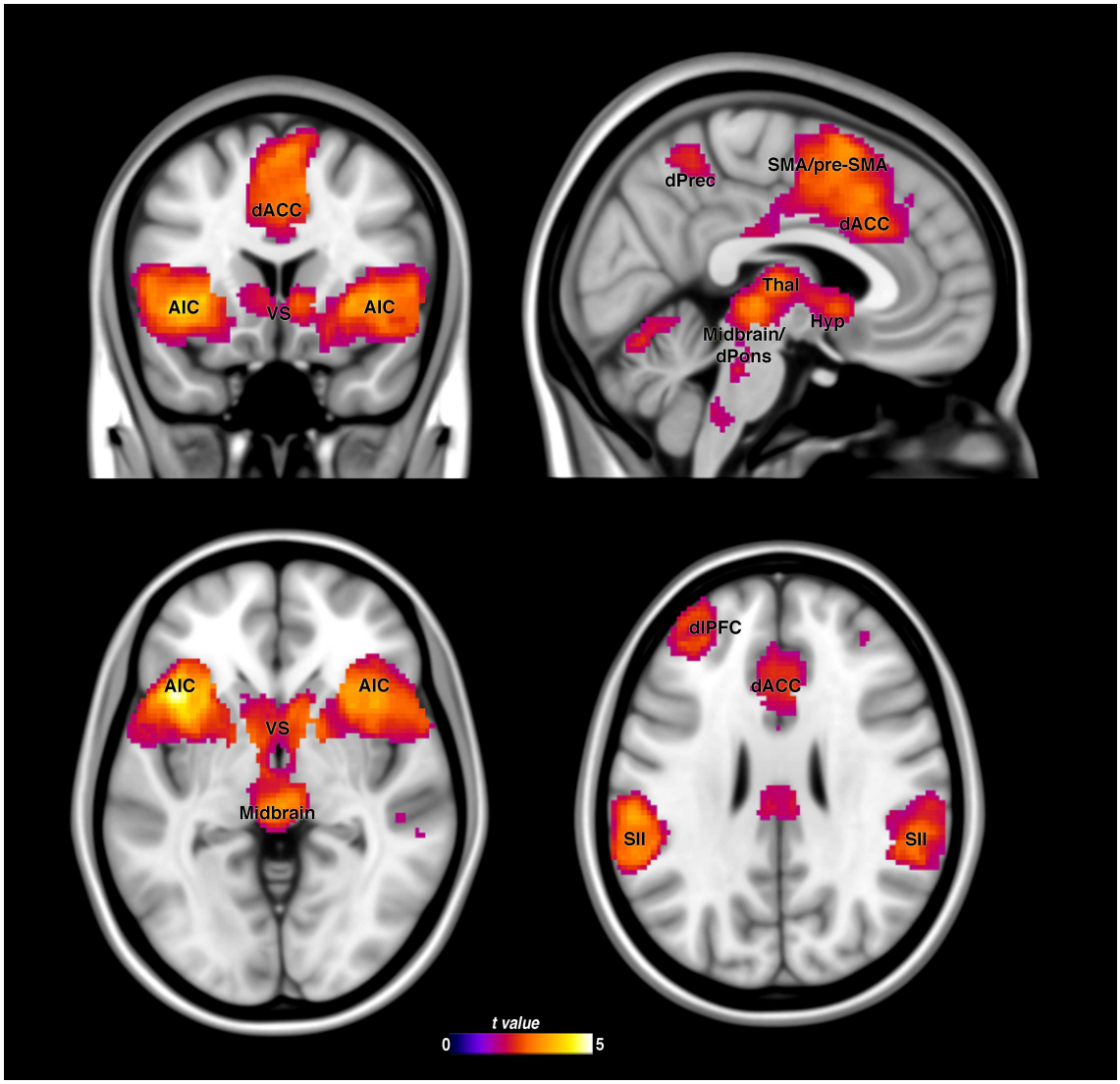

Figure 1. Significant brain functional activation to the CS+ vs. CS- determined by meta-analysis. AIC: anterior insular cortex; dACC: dorsal anterior cingulate cortex; dlPFC: dPons: dorsal pons; dPrec: dorsal precuneus; dorsolateral prefrontal cortex; PMJ: pontomedullary junction; SII: secondary somatosensory cortex; SMA: supplementary motor area; Thal: thalamus; VS: ventral striatum; HYP: hypothalamus. Results are displayed at $p < 0.005$ (cluster size $\geq$10 voxels) on the MNI 152 T1 0.5mm template.

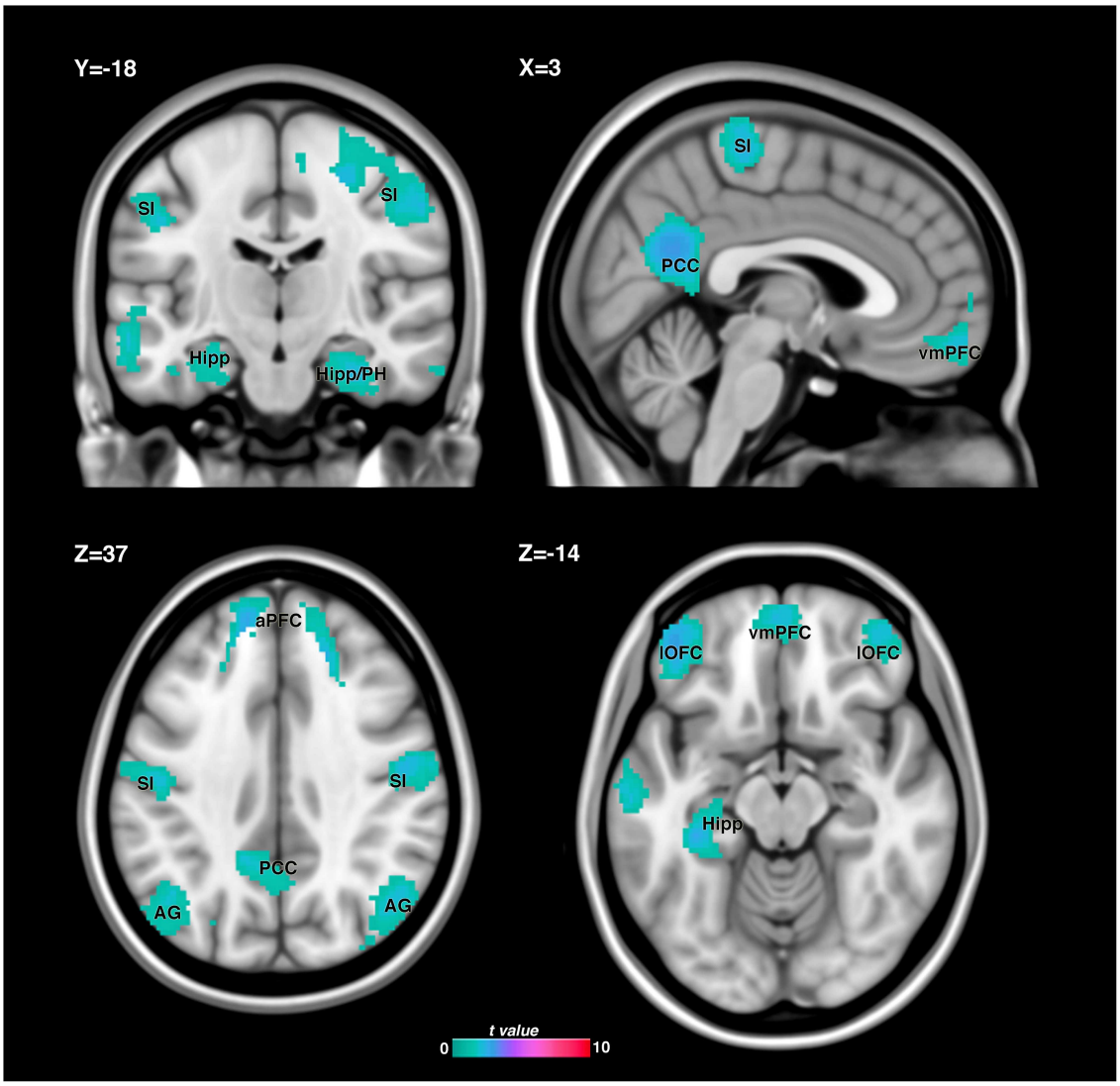

Figure 2. Significant brain functional deactivation to the CS+ vs. CS- determined by meta-analysis. AG: angular gyrus; aPFC: anterior prefrontal cortex; Hipp: hippocampus; lOFC: lateral orbitofrontal cortex; PCC: posterior cingulate cortex; PH: parahippocampal formation; SI: primary somatosensory cortex. Results are displayed at $p < 0.005$ (cluster size ≥10 voxels) on the MNI 152 T1 0.5mm template.

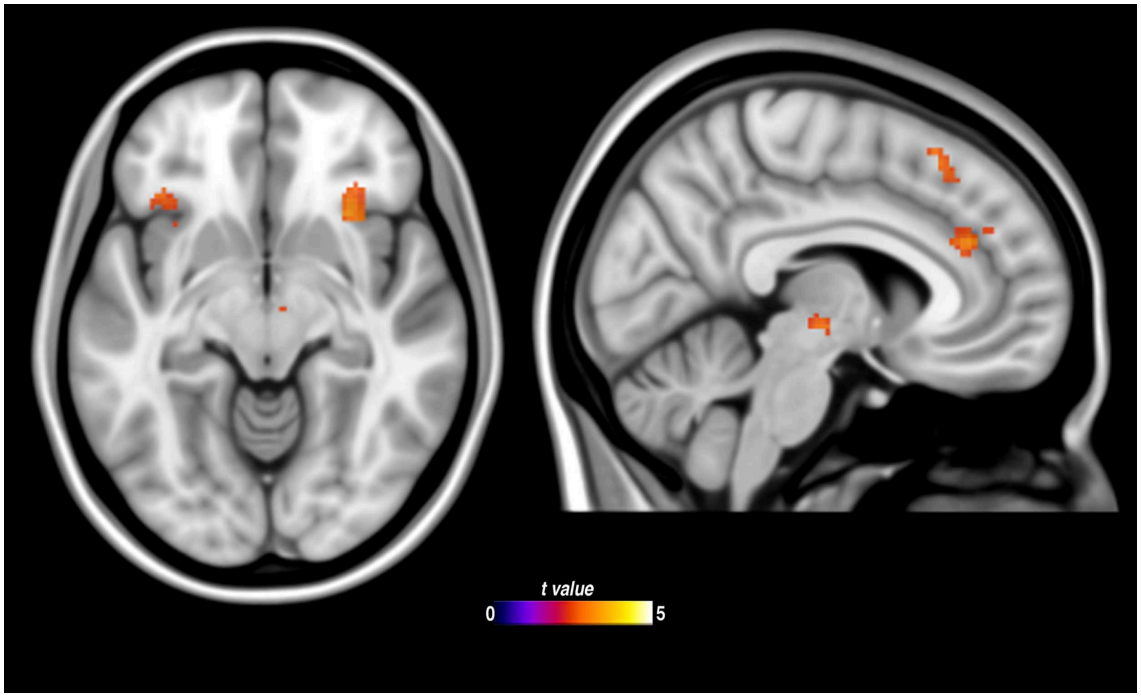

Figure 3. Influence of potential US confounding on fear conditioned brain activation, highlighting regions that demonstrated greater relative activation when no potential confounding existed. Results are displayed at $p < 0.005$ (cluster size ≥10 voxels) on the MNI 152 T1 0.5mm template.

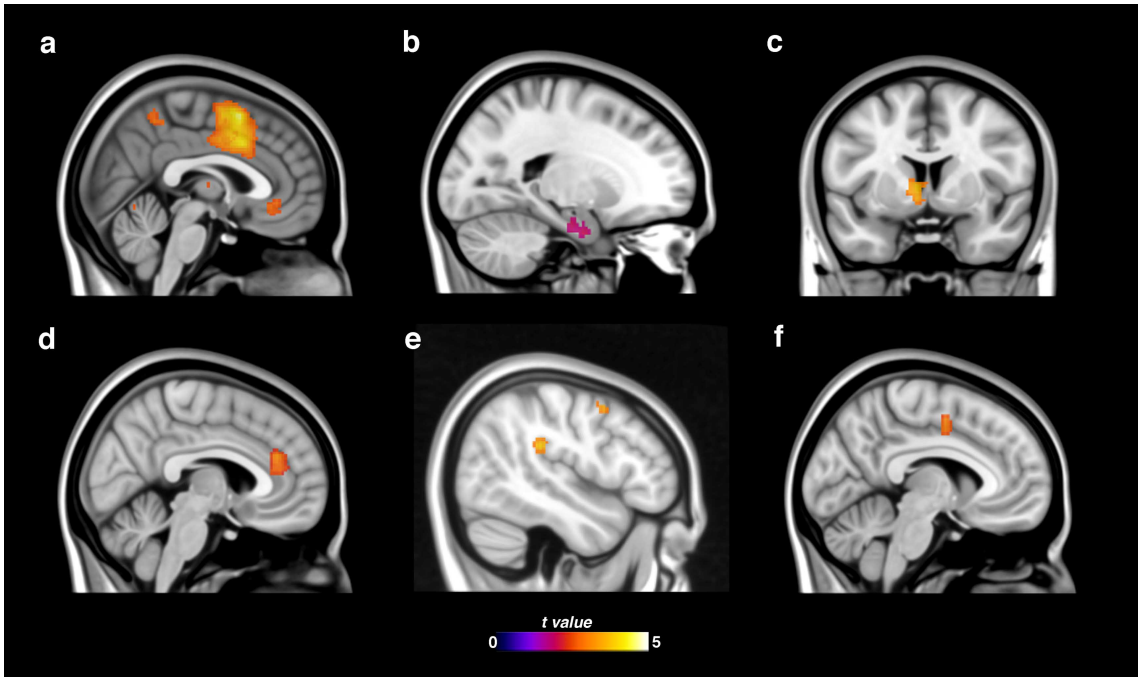

Figure 4. Summary of meta-regression analyses: influence of certain task features on fear conditioning-related brain functional activation. a) Regions exhibiting reduced activation during fear conditioning following the use of a pre-conditioning task phase; b) Regions exhibiting greater activation during fear conditioning following the use of a pre-conditioning task phase; c) Regions exhibiting greater activation during fear conditioning in relation to a higher number of presented CS trials; d) Regions exhibiting reduced activation during fear conditioning in relation to a higher CS-US reinforcement rate; e) Regions exhibiting greater activation during fear conditioning in relation to a longer CS-US delay; f) Regions exhibiting greater activation during fear conditioning in response to a tactile (electric shock) US compared to other US stimulus types. Results are displayed at $p < 0.005$ (cluster size $\geq$10 voxels) on the MNI 152 T1 0.5mm template. Because all results correspond to changes in activation levels, a warm color display has been used and a uniform activation magnitude (SDM Z) adopted for each result. Up/down arrows indicate relative increases or decreases in activation effects.

Table 1. Characteristics of the 27 delay fear conditioning fMRI datasets included in the meta-analysis.

Author, year	N	% males	Mean age	Pre-conditioning?	CSs types	Number of CS+/CS- trials[1]	Average ITI (s)	Reinforcement rate	Type of CS	CS	Type of US/ location	Average CS-US onset delay (ms)	Task? [2]	Independent assessment of conditioning	CS+>CS- analysis[3]	CS+<CS- analysis[3]	US confounding
[4]Andreatta, 2012[52]	14	50	22,8	NO	1 CS+, 1 CS-	16/16	20	100%	Visual	Neutral pictures	Shock/ left hand	10000	NO	Subjective ratings	whole	whole	NO
Dunsmoor, 2011[53]	14	50	22,6	YES	1 CS+, 1 CS-	16/16	11	63%	Visual	Fearful faces	Shock/ right wrist	4000	YES	SCR	whole	whole	-
*Eippert, 2012[54]	32	100	26,4	NO	1 CS+, 1 CS-	10/10	7,5	100%	Visual	Abstract figures	Shock/ right hand	4700	YES	SCR,HR Subjective ratings	whole	NA	-
Haritha, 2013[55]	25	36	20	NO	1 CS+, 1 CS-, other	24/24	20	100%	Auditory	Tones	Auditory	variable	NO	SCR	whole	NA	YES
*Harrison, 2014[56]	31	29	22,4	NO	1CS+, 1 CS-	16/16	6,01	50%	Visual	Neutral pictures	Auditory	1900	NO	Subjective ratings	whole, early, late	whole, early, late	NO
Hermann, 2012[57]	74	50	24,3	NO	1 CS+, 1 CS-	20/20	12	100%	Visual	Neutral pictures	Shock/ left shin	7900	NO	SCR	early	early	YES
Holt, 2012[46]	17	100	34,2	YES	2 CS+, 1 CS-	16/16	15	60%	Visual	Neutral pictures	Shock/ dominant hand	6000	NO	SCR	early, late	NA	YES
[5]Kalisch, 2009[58]	16	0	26	YES	1 CS+, 1 CS-	15/15	9	80%	Visual	Angry faces	Shock/ right hand	6250	YES	SCR	early	NA	-
Kattoor, 2013[59]	19	68	23,7	NO	1 CS+, 1 CS-	16/16	20	75%	Visual	Neutral pictures	Rectal distension	9600	NO	Subjective ratings	early, late	early, late	YES
*Klucken, 2012[60]	20	50	23,4	NO	1 CS+, 1 CS-	21/21	14	100%	Visual	Neutral pictures	Picture	8000	YES	SCR Subjective ratings	whole	NA	-
Knight, 2009[61]	15	47	28,8	NO	1 CS+, 1 CS-	60/60	20	100%	Auditory	Tones	Auditory	10000	NO	SCR Subjective ratings	whole	NA	YES
[4]Maier, 2012[62]	17	41	31	YES	1 CS+, 1 CS-	12/12	15	50%	Visual	Neutral pictures	Shock/ right wrist	5000	NO	SCR Subjective ratings	whole	whole	NO
*Menon, 2007[63]	12	67	36,5	YES	1 CS+, 1 CS-	45(30)/30	8,8	33%	Visual	Neutral pictures	Shock/ left hand	5000	NO	SCR Subjective ratings	whole	NA	NO
*Merz, 2013[64]	48	50	22,3	NO	1 CS+, 1 CS-	21/21	12	100%	Visual	Neutral pictures	Shock/ left shin	7900	YES	SCR	early, late	NA	-
*Merz, 2014[65]	32	100	24,9	NO	1CS+, 1CS-	16/16	10,75	63%	Visual	Neutral pictures	Shock/ left shin	7900	NO	SCR	early, late	NA	YES
Milad, 2007[66]	14	NA	NA	YES	2 CS+, 1 CS-	16/16	15	60%	Visual	Neutral pictures	Shock/ hand	6000	NO	SCR	early, late	early	NO
Milad, 2013[67]	17	47	25,8	YES	2 CS+, 1 CS-	16/16	15	62%	Visual	Neutral pictures	Shock/ hand	6000	NO	SCR	whole	NA	YES
*Romaniuk, 2010[68]	20	70	35,1	NO	1 CS+, 1 CS-	24 (12)/24	11	50%	Visual	Neutral pictures	Picture	2000	YES	SCR, RT	early	NA	-
Schiller, 2008[43]	17	53	22,6	NO	1 CS+, 1 CS-	18(12)/12	12	33%	Visual	Angry face	Shock/ right wrist	4000	NO	SCR	whole, early, late	NA	NO

Schultz, 2012[69]	27	56	22,3	NO	1 CS+, 1 CS-	10/10	20	100%	Visual	Neutral pictures	Shock/ right foot	8000	NO	SCR Subjective ratings	whole	NA	YES
[5]Sehlmeyer, 2011[70]	32	38	23,6	YES	1 CS+, 1 CS-	40 (30)/30	11,5	25%	Visual	Neutral faces	Auditory	2000	NO	Subjective ratings	whole	NA	NO
*Spoormaker, 2012[71]	35	100	24,2	NO	2 CS+, 1 CS-	30 (15)/15	9	50%	Visual	Neutral pictures	Shock/ right hand	3100	NO	SCR	whole	NA	NO
*Stark, 2006[72]	17	47	23,6	NO	1 CS+, 1 CS-	30/30	10	100%	Visual	Neutral pictures	Shock/ left shin	7900	NO	SCR	whole	NA	YES
*Tabbert, 2005[73]	18	6	25,2	NO	1 CS+, 1 CS-	30/30	10	100%	Visual	Neutral pictures	Shock/ left shin	7900	NO	SCR	early, late	NA	YES
*van Well, 2012[40]	37	35	22,3	NO	1 CS+, 1 CS-	8/8	20	75%	Visual	Fear pictures	Shock/ right shin	9500	NO	Startle pot. Subjective ratings	whole	whole	YES
*Visser, 2011[74]	19	26	22,2	NO	2 CS+, 2 CS-	26/26	21,5	50%	Visual	Neutral pictures	Shock/ right shin	6500	NO	Contingency awareness	whole	whole	NO
*Visser, 2013[75]	38	39	23,6	NO	2 CS+, 2 CS-, 2 CS neutral	26/26	19,5	50%	Visual	Neutral pictures	Shock/ right shin	4500	NO	Pupil dilation response	whole	whole	NO
TOTAL/MEAN	**677**	**53 %**	**25,37**			**20/20**	**13,91**	**71 %**				**5385**					

* Datasets for which statistical parametric maps were available.

[1] In parentheses, unreinforced CS trials. **[2]** Studies using a task during fear conditioning. **[3]** Contrast available for fear conditioning: whole (whole conditioning), early (early conditioning trials), late (late conditioning trials). [4] Studies where the CS+ vs. CS- contrast was calculated during a "test phase" immediately after conditioning. [5] Two fear conditioning phases were reported. In the Kalisch *et al.* study, only the first conditioning phase was included because it was followed by a fear extinction phase. In the Sehlmeyer *et al.* study, both conditioning phases were combined together.

Abbreviations: CS: Conditioned Stimulus; CS+: CS followed by unconditioned stimulus; CS-: CS not followed by unconditioned stimulus; ITI: Inter-trial interval; US: Unconditioned Stimulus; NA, not available; SCR: Skin Conductance Recording; HR: Heart Rate; RT: Reaction Time. Pot: startle potentiation; US confound: possible confounding effects of US on fMRI analyses;"-" refers to studies using cognitive tasks, which where not included in the US confound analyses.

NEURAL SIGNATURES OF HUMAN FEAR CONDITIONING: AN UPDATED AND EXTENDED META-ANALYSIS OF FMRI STUDIES

Fullana et al.

SUPPLEMENTARY MATERIAL
Figures

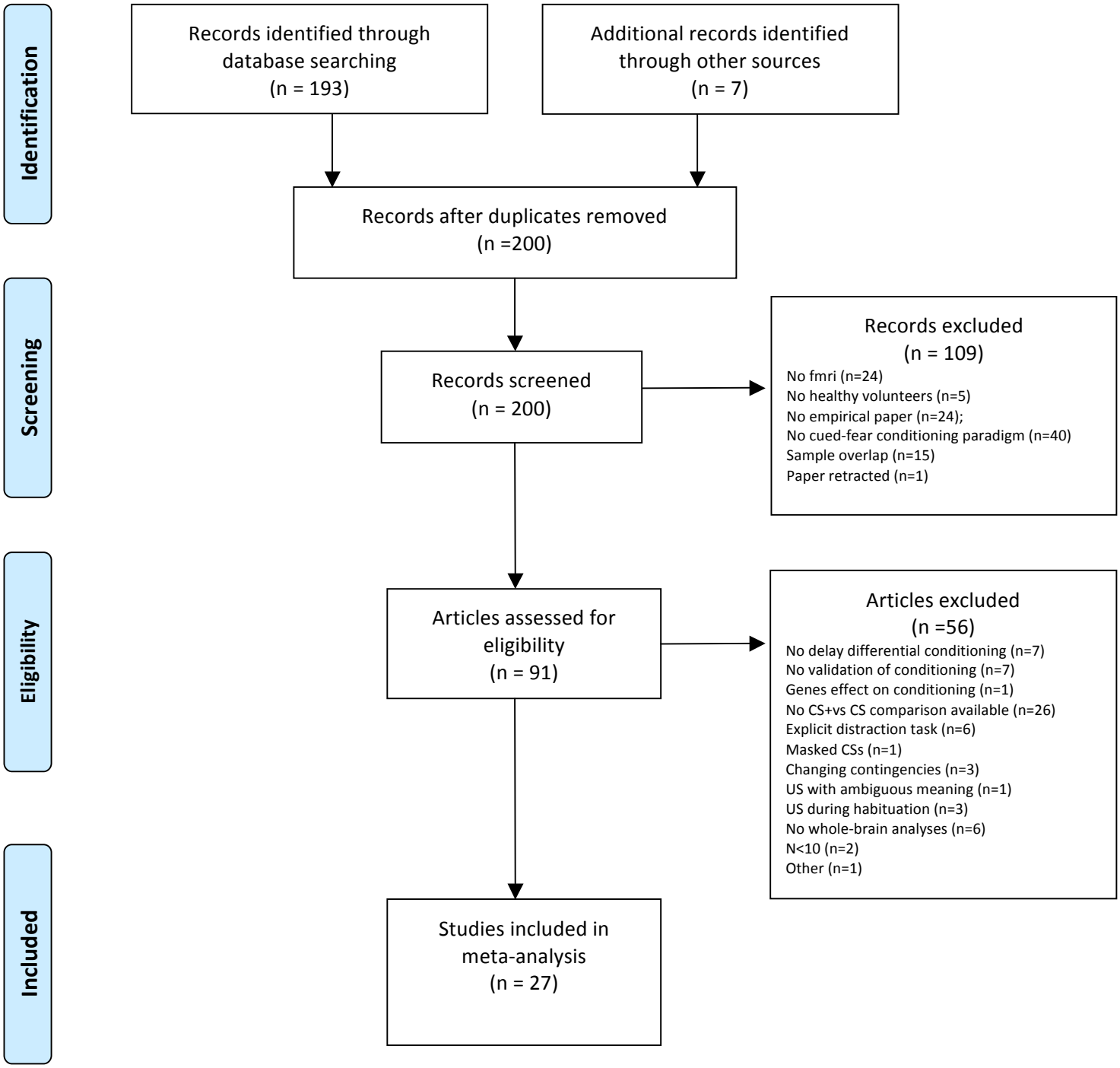

Figure 1S. PRISMA flow diagram.

Note: PRISMA=Preferred reporting items for systematic reviews and meta-analyses (http://www.prismastatement.org/).

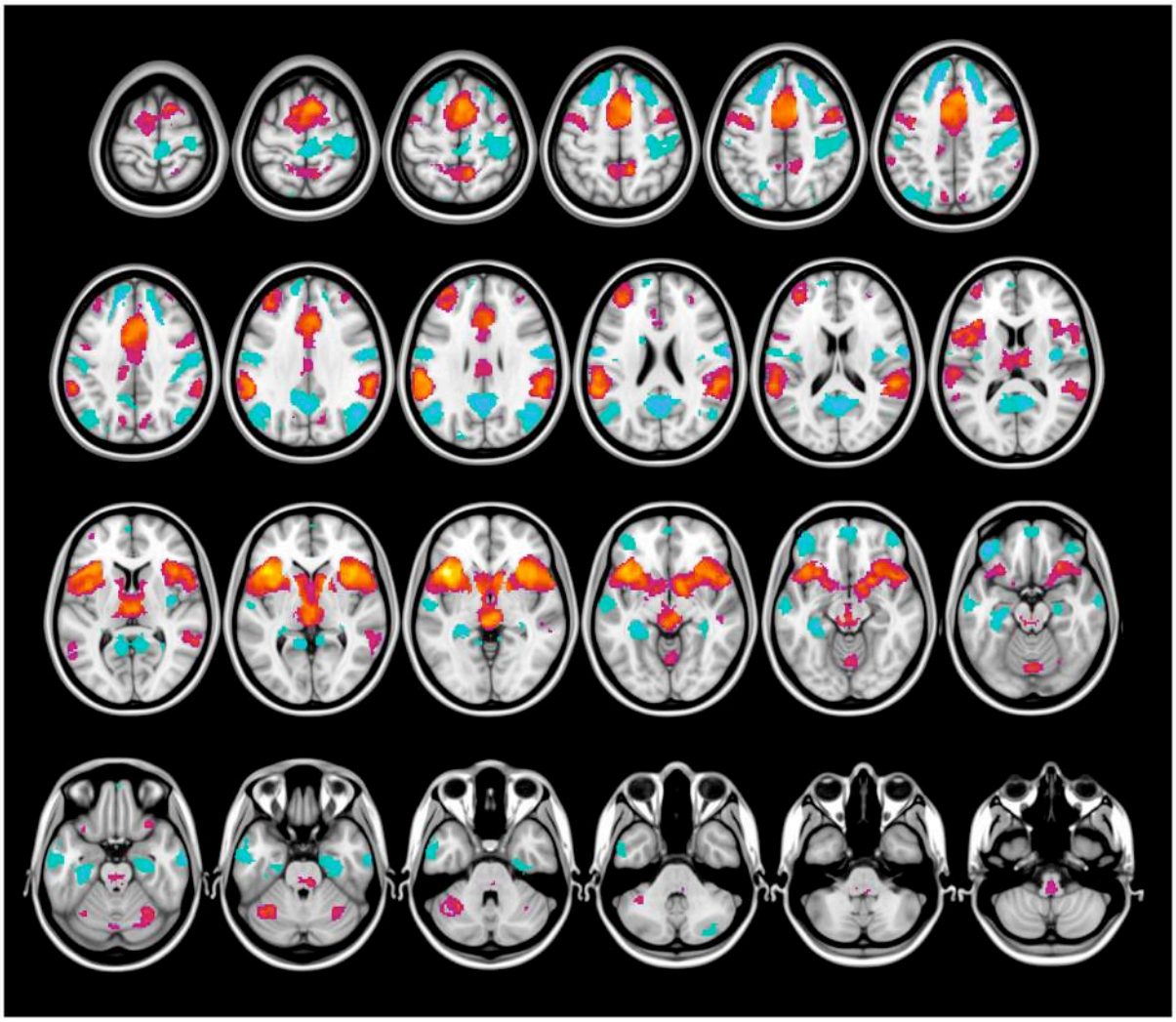

Figure 2S. Significant brain functional activation and deactivation to the CS+ vs. CS- determined by meta-analysis and displayed on 24 axial slices of the whole brain volume. Results are displayed at $p < 0.005$ (cluster size $\geq$10 voxels) on the MNI 152 T1 0.5mm template.

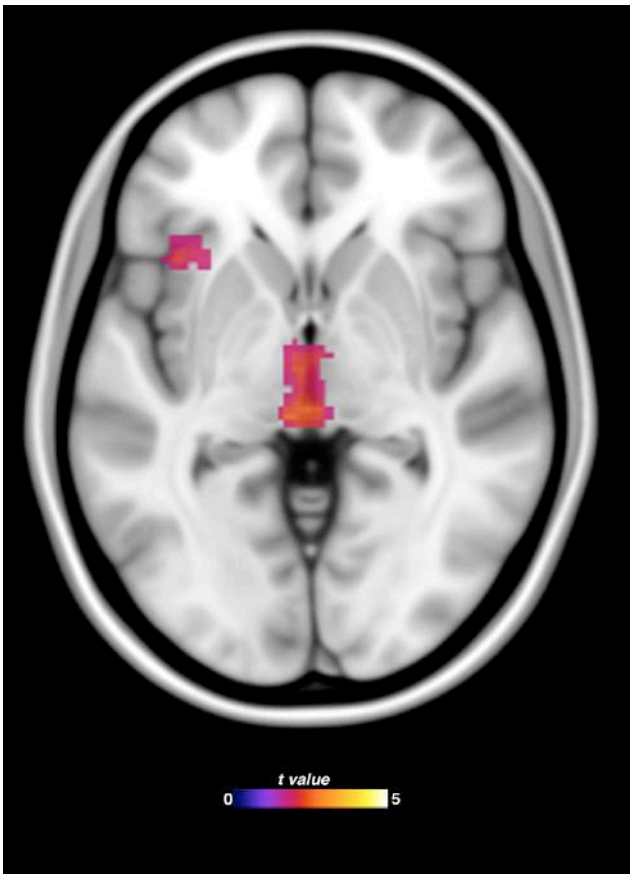

Figure 3S. Comparison of brain activation during “early” versus “late” phases during fear conditioning determined by meta-analysis highlighting regions that demonstrated greater relative activation during “early” phases. Results are displayed at $p < 0.005$ (cluster size $\geq$10 voxels) on the MNI 152 T1 0.5mm template.

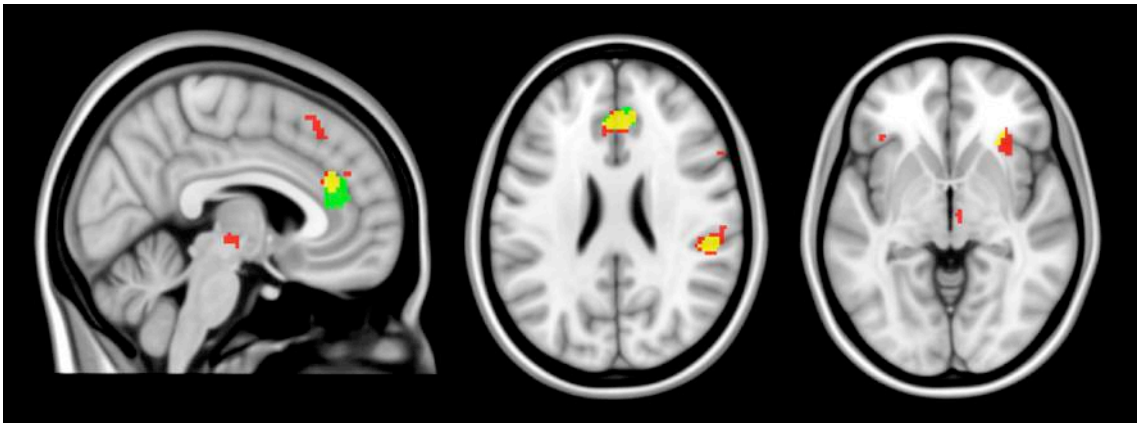

Figure 4S. Relative anatomical overlap (yellow blobs) between brain regions demonstrating greater activation during pure CS+ anticipatory trials (i.e., no potential US confounding; red blobs) and regions whose activation was modulated by reinforcement rate (i.e., higher reinforcement rate, less activation; green blobs) – possibly reflecting a common influence of stimulus uncertainty or unpredictability. Results are displayed at $p < 0.0005$ (cluster size $\geq$10 voxels) on the MNI 152 T1 0.5mm template.

NEURAL SIGNATURES OF HUMAN FEAR CONDITIONING: AN UPDATED AND EXTENDED META-ANALYSIS OF FMRI STUDIES

Fullana et al.

SUPPLEMENTARY MATERIAL
Tables

Table 1S. Activation/deactivation peaks for the included datasets (n=27)

Authors	Coordinates system	Contrast	ACTIVATIONS						DEACTIVATIONS					
			x	y	z	(peak) Z	(peak) T	(peak) p	x	y	z	(peak) Z	(peak) T	(peak) p
Andreatta et al., 2012	MNI	whole	20	-34	-10		6,06	0.000	12	-90	24		5,39	
			14	-28	-14		5,8	0.000	-28	-2	34		5,2	
			6	-30	-18		4,55	0.000	24	-12	24		5,03	
			-38	12	-24		5,49	0.000						
			-32	4	-22		4,54	0.000						
			-18	-28	-14		4,9	0.000						
			32	0	-20		4,69	0.000						
			2	-14	-44		4,62	0.000						
			-6	-38	-16		4,46	0.000						
			-34	16	-16		4,34	0.000						
			-30	-28	8		4,31	0.000						
Dunsmoor et al., 2011	MNI	whole	10	4	2		6,89		-2	32	-6		4,11	
			-10	0	14		4,69		-6	44	10		4,11	
			2	-36	-46		5,77							
			-6	-20	-2		5,35							
			34	12	6		4,61							
			-34	16	6		4,02							
			42	-8	54		4,27							
			10	-48	62		4,02							
			-30	-32	46		3,82							
Eippert et al., 2012	MNI	whole							SPM					
Haritha et al., 2013	Talairach	whole	-41,1	22,7	26,7		3,21					Not reported		
			35,7	24,3	30,6		3,16							
			-0,5	3,8	47,8		3,09							
			44,3	-52,7	37,6		2,91							
			-40,2	10,7	4,8		4,29							
			40,7	11,5	4,5		4,46							
			1,4	-33,2	26,5		3,07							
			-46,6	-28,7	15,1		3,9							
			53,7	-34,8	3,7		3,08							
			7,9	-77	4,7		3,9							
			-1,1	-58,7	-23,2		3,36							
			11,6	9,5	10,2		3,21							
			-21,9	2,5	4		3,83							
			20,6	5,6	3,4		3,28							
			-11,3	-18,3	7,3		4,98							
			11,1	-18,8	7,1		4,43							
Harrison et al., 2014	MNI	whole							SPM					
		early							SPM					
		late							SPM					
Hermann et al., 2012	MNI	early	-3	5	52		10,36					None significant		
			6	8	40		9,32							
			15	2	67		8,68							

			-39	14	4		9,08	
			-33	23	4		7,74	
			-48	8	7		7,5	
			-57	-37	25		8,07	
			-66	-31	19		7,82	
			-45	-31	13		6,13	
			63	-40	25		8	
			48	-40	19		7,43	
			57	-40	10		7	
			-45	-1	49		7,64	
			-30	-1	55		5,38	
			-15	-76	31		7,63	
			-15	-85	19		6,11	
			-24	-64	7		6,09	
			0	-49	52		7,56	
			18	-40	70		7,48	
			9	-55	52		6,89	
			33	17	7		7,14	
			51	5	1		6,81	
			18	14	-5		6,77	
			0	-34	-38		6,91	
			3	-28	-26		5,9	
			0	-64	-5		6,72	
			0	-73	-11		6,46	
			27	-64	-20		5,74	
			-9	-25	-8		6,66	
			-6	-25	4		6,3	
			6	-25	4		5,42	
			-36	-55	-29		6,59	
			-30	-61	23		5,67	
			18	-37	7		6,45	
			15	-76	37		6,07	
			21	-70	25		5,21	
			-24	-46	64		5,99	
			-33	44	28		5,92	
			-36	53	16		5,43	
			15	-49	-29		5,84	
			-12	-34	43		5,51	
			-12	-25	46		5,39	
Holt et al., 2012	MNI	early	-10	-21	-7	5,51	0,00000004	Not reported
			42	-85	-8	5,21	0,0000002	
			-20	-14	-24	4,53	0,000036	
			-50	-55	-17	4,44	0,000009	
			32	-56	-12	4,06	0,00005	
			-38	13	-1	3,62	0,0012	
		late	20	-34	-1	3,89	0,0004	
Kalisch et al., 2009	MNI	early	-18	0	-36			Not reported
			-32	6	-48			
			-18	-2	-10			
			32	-10	-40			
			30	4	-50			

			20	-6	-38						
			36	20	-42						
			60	8	-36						
			50	-78	-4						
Kattoor et al., 2013	MNI	early	20	-70	-12	6,47					None significant
			32	-68	-16	5,1					
			6	-72	-10	4,2					
			42	-6	-20	5,1					
			4	-90	16	5,09					
			8	-82	18	3,97					
			4	-52	70	5,08					
			2	30	-2	4,95					
			28	6	-12	4,74					
			30	4	-2	3,89					
			4	-54	18	4,71					
			-5	-55	14	3,8					
			44	-28	-14	4,63					
			-32	12	-28	4,5					
			-28	-24	6	4,42					
			34	44	42	4,4					
			-18	-50	-16	4,37					
			-20	-76	-20	4,27					
			50	-14	6	4,25					
			-38	-50	-26	4,25					
			-28	-62	-16	4,22					
			-22	-50	-26	4,19					
			-22	-54	24	4,18					
			44	-46	10	4,1					
			30	26	-12	4,07					
			54	-38	8	4,06					
			-30	2	-2	3,95					
			12	42	4	3,94					
			-14	-80	10	3,91					
			26	-64	8	3,89					
			22	42	-2	3,82					
			-22	-60	-32	3,78					
			-34	-18	4	3,76					
			-30	-46	-30	3,75					
			-18	-60	-30	3,74					
			2	-86	34	3,73					
			-2	-70	-12	3,7					
			-30	-2	4	3,7					
			-24	-10	8	3,69					
			10	-60	-40	3,69					
			-12	40	-2	3,69					
			12	-72	12	3,68					
			30	2	-6	3,68					
			-14	36	-2	3,66					
			-22	-48	8	3,66					
		late	24	2	-22	3,89					
Klueken et al., 2012	MNI	whole					SPM	60	-6	16	3,76

Knight et al., 2009	Talairach	whole				F value				Not reported	
			22	-6	13	30.31					
			41	-20	22	31.09					
			-6	-72	31	28.66					
			-8	1	8	34.61					
			15	-61	-24	31.17					
			-18	-21	60	30.71					
Maier et al., 2012	MNI	whole	3	35	37	5,02	-12	-52	10		3,7
			-30	23	-5	6,04	12	-52	10		4,05
			30	23	-8	6,25	-18	35	43		3,99
			12	20	64	4,03	24	29	43		4,63
			-60	-46	34	4,67	-24	-37	-14		4,03
			63	-46	28	3,96	27	-19	-20		4,39
			6	-22	1	4,05	36	-10	16		5,25
							45	-70	28		4,66
							-27	-76	37		3,74
							30	-79	40		3,77
							6	-34	61		4,13
							-54	-16	43		4,17
							51	-13	55		5,05
							-6	44	-20		4,58
							-45	-7	-23		3,8
							60	-7	-23		4,27
							-54	-4	-11		3,73
							-6	44	-20		4,58
Menon et al., 2007	MNI	whole					SPM				
Merz et al., 2013	MNI	early					SPM				
		late					SPM				
Merz et al, 2014	MNI	early					SPM				
		late					SPM				
		early vs late					SPM				
Milad et al., 2007b	MNI	early			None significant		8	31	-14		0,000072
Milad et al., 2013	MNI	whole	-18	-100	4	10,43				Not reported	
			14	-84	6	9,22					
Romaniuk et al, 2010	MNI	early					SPM				
Schiller et al., 2008	MNI	whole	12	3	10	8,589				Not reported	
			-8	3	8	6,745					
			22	5	-2	6,766					
			-27	1	8	6,006					
			46	6	5	8,39					
			-33	20	4	6,588					
			9	-13	1	5,962					
			-9	-23	-11	5,118					
			3	32	16	5,113					
			0	14	29	5,773					
			1	0	43	7,107					
			6	-53	47	4,27					
			-10	-37	40	4,603					
			54	-24	24	6,297					
			-48	-28	20	8,504					
			-31	-46	-23	6,504					

		early	10	2	10	6,149	Not reported
			-8	3	10	4,503	
			24	4	-1	6,683	
			-25	-3	7	5,138	
			46	8	5	7,305	
			-48	2	8	6,472	
			9	-12	1	4,598	
			6	-10	-5	4,52	
			-9	-10	-6	4,319	
			-7	-25	-10	4,787	
			0	15	26	5,37	
			0	-7	61	6,821	
			6	-57	47	4,947	
			-9	-37	41	4,611	
			57	-28	25	6,256	
			-53	-33	23	6,84	
			-13	-44	-13	6,559	
		late	14	2	10	6,604	Not reported
			-8	3	7	5,118	
			-26	3	4	4,923	
			40	9	10	5,485	
			-36	9	11	6,127	
			15	-14	0	3,829	
			-12	-16	11	3,874	
			-2	-25	-17	3,939	
			-2	35	16	3,561	
			-3	0	46	3,972	
			-5	-9	65	4,987	
			43	-25	25	2,697	
			-50	-27	20	4,052	
			32	-46	-23	4,199	
Schultz et al. 2012	Talairach	whole	0	-23	12		Not reported
			6	-58	0		
			-20	-12	69		
			1	4	48		
			2	-55	63		
			-60	-19	21		
			-20	0	-7		
			-45	-31	57		
			-49	11	1		
			34	-7	60		
			50	19	-5		
Sehlmeyer et al., 2011	MNI	whole	-10	8	-4	5,32	Not reported
			16	18	54	5,12	
			6	38	20	4,61	
			46	-36	24	4,59	
			28	26	-6	4,56	
			0	-84	-6	4,5	
			20	12	36	4,26	
			34	-78	14	4,02	
			-36	-6	-22	3,9	

			18	-2	2	3,88	
			-60	-42	10	3,87	
			20	-46	54	3,75	
			50	10	48	3,75	
			-36	22	4	3,73	
			28	-68	-10	3,56	
			-48	-22	-10	3,54	
			18	-44	40	3,48	
			-32	44	28	3,35	
			-60	-38	30	3,33	
Spoormaker et al., 2012	MNI	whole					SPM
Stark et al., 2006	MNI	whole					SPM
Tabbert et al., 2005	MNI	early					SPM
		late					SPM
van Well et al., 2012	MNI	whole					SPM
Visser et al., 2011	MNI	whole					SPM
Visser et al., 2013	MNI	whole					SPM

Abbreviations: MNI: Montreal Neurological Institute space; SPM: Statistical Parametrical Map.
See references in main text.

Table 2S. Results of meta-analysis for the CS+ > CS- and CS+ < CS- contrasts during fear conditioning: regional differences in activation at p<0.005, z>1 and cluster size >10 voxels.

Finding	Cluster description			Local peaks and breakdown							
	Brain region (subcluster)	Number of voxels	*Cluster P* (GRF)	MNI	SDM-Z	*Voxel P* (unc)	I^2	JK	Egger test P	Brain region	Number of voxels
CS+ > CS- (activations)											
Bilateral insula, basal ganglia and thalamus	Bilateral insula, basal ganglia and thalamus	9736	<0.000001								
	(left insula)			-40,18,-2	9.700	<0.000001	12%	27 / 27	0.177	Left insula BA 48, 47	957
				-46,2,10	5.525	<0.000001				Left rolandic operculum BA 48, 6	248
				-16,6,-14	4.824	0.00001				Left olfactory cortex BA 48, 25	60
				-52,6,-8	4.425	0.00008				Left superior temporal gyrus BA 38, 48	282
				-24,26,-10	3.771	0.001				Left inferior frontal gyrus BA 47, 48	1045
										Left superior frontal gyrus BA 48	18
										Left precentral gyrus BA 6	15
	(right insula)			40,16,2	7.488	<0.000001	8%	27 / 27	0.234	Right insula BA 48, 47	955
				52,16,4	6.293	<0.000001				Right inferior frontal gyrus BA 47, 48	999
				54,10,-8	5.706	<0.000001				Right superior temporal gyrus BA 38, 48	198
										Right rolandic operculum BA 48, 6	180
										Right olfactory cortex BA 48, 25	73
										Right gyrus rectus BA 11	18
										Right superior frontal gyrus BA 11	11
	(right basal ganglia)			28,20,-2	6.838	<0.000001	13%	27 / 27	0.333	Right putamen	202
				12,4,-6	6.511	<0.000001				Right pallidum	89
				6,12,-4	5.597	<0.000001				Right caudate nucleus	201
	(right thalamus)			2,-18,6	6.655	<0.000001	0%	27 / 27	0.092	Right thalamus	309
	(left thalamus)			-2,-18,4	6.621	<0.000001	0%	27 / 27	0.129	Left thalamus	434
										Vermis	14
	(left basal ganglia)			-12,0,-6	5.414	<0.000001	7%	27 / 27	0.473	Left pallidum	69
				-20,10,2	5.034	<0.000001				Left putamen	254
				-4,12,2	4.465	0.00007				Left caudate nucleus	182
										Right putamen	14
Bilateral supplementary motor area and precuneus	Bilateral supplementary motor area and precuneus	5829	<0.000001								

		(right supplementary motor area)			10,6,50	7.104	<0.000001	12%	27 / 27	0.011	Right supplementary motor area BA 6, 8	1085
					8,18,42	6.707	<0.000001				Right median cingulate gyrus BA 24, 32	728
											Right anterior cingulate gyrus BA 24, 32	121
					16,-2,60	4.700	0.00002				Right superior frontal gyrus BA 6, 8	210
		(left supplementary motor area)			-4,18,42	6.086	<0.000001	5%	27 / 27	0.189	Left superior frontal gyrus BA 6, 32	272
					-2,16,54	6.311	<0.000001				Left supplementary motor area BA 6, 32	1236
					-10,6,44	6.280	<0.000001				Left median cingulate gyrus BA 24, 23	731
											Left anterior cingulate gyrus BA 24, 32	270
											Left paracentral lobule BA 6	19
											Left precentral gyrus BA 6	12
		(left precuneus)			-6,-52,54	5.040	<0.000001	0%	27 / 27	0.000	Left precuneus BA 5, 7	246
					-24,-44,56	3.869	0.0008				Left postcentral gyrus	11
		(right precuneus)		(0.0003)	10,-52,56	6.113	<0.000001	0%	27 / 27	0.006	Right precuneus BA 5, 7	366
					18,-50,66	4.168	0.0002				Right superior parietal gyrus BA 5, 2	52
											Right paracentral lobule	12
Bilateral supramarginal	Right supramarginal		2008	<0.000001	54,-36,16	6.348	<0.000001	0%	27 / 27	0.007	Right superior temporal gyrus BA 42, 22	593
					58,-36,32	5.964	<0.000001				Right supramarginal gyrus BA 48, 40	861
					60,-48,10	4.915	0.000007				Right middle temporal gyrus BA 22, 21	355
					44,-28,22	3.755	0.001				Right rolandic operculum BA 48	53
											Right angular gyrus BA 48, 40	52
											Right inferior parietal gyri BA 40	15
	Left supramarginal		1661	0.000001	-58,-30,26	7.057	<0.000001	0%	27 / 27	0.001	Left supramarginal gyrus BA 48, 40	793
					-58,-52,10	4.093	0.0003				Left middle temporal gyrus BA 21, 37	103
											Left superior temporal gyrus BA 42, 48	503
											Left inferior parietal BA 40	90
											Left postcentral gyrus 48, 22	79
Bilateral middle frontal	Left middle frontal		961	0.00008	-36,44,22	5.635	<0.000001	2%	27 / 27	0.000	Left middle frontal gyrus BA 46, 45	931
											Left inferior frontal gyrus BA 46	15
											Left superior frontal gyrus BA 46	12
	Right middle frontal		116	n.s.	34,44,32	4.219	0.0002	0%	27 / 27	0.379	Right middle frontal gyrus BA 46, 9	113

Bilateral precentral	Right precentral	565	0.002	44,4,48	5.252	<0.000001	24%	27 / 27	0.933	Right precentral gyrus BA 6, 44	391
										Right middle frontal gyrus BA 6, 9	170
	Left precentral	529	0.002	-40,0,46	5.379	<0.000001	4%	27 / 27	0.029	Left precentral gyrus BA 6	506
										Left middle frontal gyrus BA 6	18
Bilateral precuneus	Left precuneus	76	n.s.	-12,-70,38	4.530	0.00005	3%	27 / 27	0.026	Left superior occipital gyrus	<10
										Precuneus BA 7	55
	Right precuneus	107	n.s.	12,-72,34	4.143	0.0003	8%	27 / 27	0.000	Right cuneus cortex BA 7	58
				10,-70,40	3.908	0.0007				Right precuneus BA 7	49
Cerebellum	Left cerebellum	385	0.008	-32,-62,-26	5.136	<0.000001	0%	27 / 27	0.030	Left cerebellum	375
	Bilateral cerebellum	536	0.029	32,-60,-24	5.096	<0.000001	0%	27 / 27	0.056	Right cerebellum	289
										Vermis	196
										Left cerebellum	45
CS+ < CS- (deactivations)											
Bilateral postcentral gyrus, insula and paracentral	Right postcentral gyrus, insula and paracentral	3060	n.s.								
	(right postcentral gyrus)			66,-6,24	-3.649	<0.000001	1%	27 / 27	0.419	Right postcentral gyrus BA 3, 4	1534
										Right precentral gyrus BA 6, 4	571
										Right supramarginal gyrus, BA 40	38
	(right insula)			38,-10,16	-2.584	0.000003	44%	27 / 27	0.588	Right insula BA 48	135
										Right rolandic operculum BA 48	104
	(paracentral)			2,-28,64	-2.422	0.00001	15%	27 / 27	0.371	Right paracentral lobule BA 4	284
				-8,-36,66	-1.131	0.005				Left paracentral lobule BA 4	93
				10,-20,58	-1.728	0.0004				Right supplementary motor area BA 4	78
	Left postcentral and insula	686	n.s.								
	(left postcentral gyrus)			-56,-6,22	-2.389	0.00001	27%	27 / 27	0.898	Left postcentral gyrus BA 43, 3	483
				-54,-24,44	-1.471	0.001				Left inferior parietal BA 3	44
										Left precentral gyrus BA 4	52
										Left supramarginal gyrus BA 3	13
	(left insula)			-34,-10,16	-2.340	0.00002	3%	27 / 27	0.828	Left insula BA 48	47
										Left rolandic operculum BA 48	45
Bilateral superior middle frontal	Right superior middle frontal	986	n.s.	18,34,44	-3.451	<0.000001	0%	27 / 27	0.259	Right superior frontal gyrus 9, 8	676

				30,16,50	-2.088	0.00007				Right middle frontal gyrus BA 8, 9	309
	Left superior middle frontal	1780	n.s.	-22,22,44	-2.953	0.0000004	0%	27 / 27	0.780	Left middle frontal gyrus BA 8, 9	448
				-12,44,38	-2.924	0.0000004				Left superior frontal gyrus BA 9, 8	1161
										Left gyrus rectus BA 11	58
				4,62,4	-1.258	0.003				Right superior frontal gyrus BA 11	67
										Right gyrus rectus BA 11	37
Bilateral precuneus, hippocampus / parahippocampal and middle temporal	Precuneus, left hippocampus and left middle temporal	3798	n.s.								
	(right precuneus)			2,-58,24	-3.049	<0.000001	29%	27 / 27	0.940	Right precuneus BA 23, 30	435
										Right calcarine fissure BA 17, 30	132
										Right posterior cingulate gyrus BA 23	69
										Right lingual gyrus BA 27, 30	54
										Right cuneus BA 23	17
										Right median cingulate gyrus BA 23	17
										Vermis	28
	(left hippocampus)			-32,-32,-12	-2.614	0.000002	0%	27 / 27	0.941	Left hippocampus BA 20, 37	257
				-24,-40,-6	-2.549	0.000005				Left parahippocampal gyrus BA 37, 20	219
				-34,-28,-22	-2.486	0.000007				Left fusiform gyrus BA 20, 37	191
	(left precuneus)			-10,-48,4	-2.511	0.000006	0%	27 / 27	0.640	Left calcarine fissure BA 17, 30	200
				-10,-50,34	-2.309	0.00002				Left precuneus BA 23, 30	576
										Left posterior cingulate gyrus BA 23, 30	143
										Left lingual gyrus BA 18, 27	67
										Left median cingulated gyrus BA 23	52
										Left cuneus cortex BA 23	43
	(left middle temporal)			-50,-12,-26	-2.387	0.00001	5%	27 / 27	0.818	Left inferior temporal gyrus BA 20, 21	228
				-60,-16,-14	-2.101	0.00007				Left middle temporal gyrus BA 21, 22	599
				-56,-12,-2	-1.933	0.0002				Left superior temporal gyrus BA 48, 22	87
	Right middle temporal	179	n.s.	62,-10,-24	-2.875	0.0000005	4%	27 / 27	0.354	Right middle temporal gyrus BA 21, 20	125
										Right inferior temporal gyrus BA 20, 21	54
	Right hippocampus	100	n.s.	32,-34,-6	-1.961	0.0001	0%	27 / 27	0.680	Right hippocampus BA 37, 20	61
				34,-42,-8	-1.494	0.001				Right parahippocampal gyrus 17	18
	Right parahippocampal	427	n.s.	30,-18,-26	-2.351	0.00001	27%	27 / 27	0.629	Right parahippocampal gyrus BA 20, 36	243
										Right hippocampus BA 20, 35	57
										Right fusiform gyrus BA 20	33
										Right cerebellum	11

Bilateral inferior middle frontal	Left inferior middle frontal	449	n.s.	-42,44,-14	-2.928	0.0000004	0%	27 / 27	0.464	Left inferior frontal gyrus BA 47, 11	288
				-34,40,-10	-1.610	0.0007				Left middle frontal gyrus BA 47, 11	126
	Right inferior middle frontal	197	n.s.	44,50,-12	-2.099	0.00007	0%	27 / 27	0.919	Right middle frontal gyrus BA 47	113
										Right inferior frontal gyrus BA 47	84
Bilateral angular	Left angular gyrus	1174	n.s.								
	(left angular)			-48,-62,28	-2.727	0.000001	0%	27 / 27	0.812	Left angular gyrus BA 39, 7	605
				-26,-78,42	-1.673	0.0005				Left middle occipital gyrus BA 19, 39	125
										Left inferior parietal BA 7	105
										Left middle temporal gyrus BA 39	79
	(left superior parietal)			-18,-60,48	-1.696	0.0005	0%	27 / 27	0.727	Left superior parietal gyrus BA 7	108
	(left superior occipital)			-20,-88,28	-1.503	0.001	44%	26 / 27	0.111	Left superior occipital gyrus BA 19	61
	Right angular gyrus	877	n.s.								
	(left angular)			44,-62,30	-2.681	0.000002	12%	27 / 27	0.246	Right angular gyrus BA 39, 7	485
				36,-84,34	-1.408	0.002				Right middle occipital gyrus BA 39, 19	283
				34,-78,46	-1.272	0.003				Right superior occipital gyrus BA 7	18
										Right middle temporal gyrus BA 39	36
	(right superior parietal)			22,-64,50	-1.300	0.003	3%	23 / 27	0.803	Right superior parietal gyrus	10
Right calcarine fissure	Right calcarine fissure	15	n.s.	30,-52,8	-1.883	0.0002	0%	27 / 27	0.885	Right calcarine fissure	< 10
Cerebellum	Right cerebellum	53	n.s.	30,-80,-38	-1.503	0.001	0%	27 / 27	0.951	Right cerebellum	53
Bilateral caudate	Left caudate nucleus	32	n.s.	-18,4,24	-1.826	0.0003	0%	27 / 27	0.319	Left caudate nucleus	24
	Right caudate nucleus	19	n.s.	16,-6,24	-1.333	0.002	0%	25 / 27	0.553	Right caudate nucleus	< 10
Left precuneus	Left precuneus	11	n.s.	-12,-74,60	-1.279	0.003	0%	24 / 27	0.812	Left precuneus	< 10

Only one local peak per gray matter brain region is displayed. Only the two BA with more voxels are displayed for region.
Abbreviations: GRF: Gaussian Random Field; MNI: Montreal Neurological Institute; SDM: Signed Differential Mapping; P: p-value; I^2:Percentage of variance attributable to study heterogeneity; JK, Jackknife Sensitivity Test, BA: Brodmann's area
Note: Cluster p-values refer to the GRF probability of finding clusters to that size according to the thresholds derived from the permutation test; when the maps were thresholded using threshold usual for GRF, many of the n.s. p-values became statistically significant.

Table 3S. Results of meta-analysis for the CS+ > CS- and CS+ < CS- contrasts during fear conditioning in studies with and without US confounding: regional differences in activation at p<0.005, z>1 and cluster size >10 voxels

Clusters of ≥ 10 voxels with all voxels SDM-Z ≥ 3.550

GREATER ACTIVATION WITH CONFOUNDING

MNI	*SDM-Z*	*Voxel P* (unc)	*Cluster P* (GRF)	Voxels	Description
8,-60,4	3.845	0.000124582	n.s.	29	Right lingual gyrus, BA 18

GREATER DEACTIVATION WITH CONFOUNDING

MNI	*SDM-Z*	*Voxel P* (unc)	*Cluster P* (GRF)	Voxels	Description
-28,-78,42	4.287	0.00001	n.s.	73	Left inferior parietal (excluding supramarginal and angular) gyri, BA 19
38,-26,-14	3.919	0.00009	n.s.	14	Right hippocampus, BA 20
26,-76,44	3.911	0.00009	n.s.	11	Right superior occipital gyrus, BA 7
-6,52,-14	3.789	0.0002	n.s.	13	Left superior frontal gyrus, medial orbital, BA 11

Clusters of ≥ 10 voxels with all voxels SDM-Z ≤ -2.375

GREATER ACTIVATION WITHOUT CONFOUNDING

MNI	*SDM-Z*	*Voxel P* (unc)	*Cluster P* (GRF)	Voxels	Description
48,-30,24	-3.558	0.000003	n.s.	135	Right supramarginal gyrus, BA 48
30,18,-12	-3.385	0.000006	n.s.	250	Right insula, BA 48
4,36,24	-3.361	0.000007	n.s.	149	Right anterior cingulate / paracingulate gyri, BA 32
8,24,54	-3.129	0.00002	n.s.	53	Right supplementary motor area, BA 8
-36,24,-16	-2.980	0.00004	n.s.	77	Left inferior frontal gyrus, orbital part, BA 38
-10,14,4	-2.845	0.00007	n.s.	24	Left caudate nucleus, BA 25
6,-16,-6	-2.814	0.00008	n.s.	15	(undefined)
56,18,26	-2.509	0.0003	n.s.	10	Right inferior frontal gyrus, opercular part, BA 44

Abbreviations: GRF: Gaussian Random Field

Note: Cluster p-values refer to the GRF probability of finding clusters to that size according to the thresholds derived from the permutation test; when the maps were thresholded using threshold usual for GRF, many of the n.s. p-values became statistically significant.

.

Table 4S. Results of meta-analysis for the CS+ > CS- and CS+ < CS- contrasts during fear conditioning (early versus late phases): regional differences in activation at p<0.005, z>1 and cluster size >10 voxels

Clusters of ≥ 10 voxels with all voxels SDM-Z ≥ 2.420

GREATER ACTIVATION LATE>EARLY

MNI	*SDM-Z*	*Voxel P* (unc)	*Cluster P* (GRF)	Voxels	Description
-8,28,-14	3.567	0.00004	n.s.	237	Left superior frontal gyrus, medial orbital, BA 11
18,24,-16	3.303	0.0002	n.s.	65	Right superior frontal gyrus, orbital part, BA 11
24,-4,-32	3.102	0.0004	n.s.	56	Right parahippocampal gyrus, BA 35

Clusters of ≥ 10 voxels with all voxels SDM-Z ≤ -1.809

GREATER DEACTIVATION LATE>EARLY

MNI	*SDM-Z*	*Voxel P* (unc)	*Cluster P* (GRF)	Voxels	Description
18,-60,28	-2.798	0.00008	n.s.	122	Right precuneus, BA 23

GREATER ACTIVATION EARLY>LATE

MNI	*SDM-Z*	*Voxel P* (unc)	*Cluster P* (GRF)	Voxels	Description
0,-26,-2	-2.603	0.0002	n.s.	299	(undefined)
-60,-26,28	-2.540	0.0003	n.s.	57	Left supramarginal gyrus, BA 48
-38,18,-2	-2.291	0.0008	n.s.	67	Left insula, BA 47

Abbreviations: GRF: Gaussian Random Field
Note: Cluster p-values refer to the GRF probability of finding clusters to that size according to the thresholds derived from the permutation test; when the maps were thresholded using threshold usual for GRF, many of the n.s. p-values became statistically significant.

Table 5S. Results of meta-regression analyses

Variable	Cluster description			Local peaks and breakdown				
	Brain region	Number of voxels	*Cluster P* (GRF)	MNI	SDM-Z	*Voxel P* (unc)	Brain region	Number of voxels
Percentage of males								
(none)								
Mean age								
↓ deactivation with age	Left hippocampus	88	n.s.	-30,-16,-28	2.973	0.00001	Left fusiform gyrus BA 20, 36	37
				-18,-16,-24	2.498	0.0001	Left parahippocampalgyrus BA 36	32
							Left hippocampus	14
↓ activation with age	Right insula	200	n.s.	46,12,2	-3.235	0.000001	Right insula BA 48, 47	118
							Right inferior frontal gyrus	71
↓ activation with age	Right supplementary motor area	81	n.s.	4,12,54	-2.830	0.00004	Right supplementary motor area BA 6, 32	65
							Left supplementary motor area	16
↓ activation with age	Left insula	20	n.s.	-56,6,10	-2.655	0.0001	Left inferior frontal gyrus	<10
							Left rolandic operculum BA 48	13
Habituation								
↑ activation	Left parahippocampal	153	n.s.	-22,-6,-30	2.114	0.0001	Left parahippocampalgyrus BA 36, 28	111
							Left hippocampus BA 35	29
	Left superior temporal	11	n.s.	-46,-22,-8	1.979	0.0002	(undefined)	
	Right postcentral	11	n.s.	66,-8,22	1.959	0.0002	Right postcentralgyrus BA 43	11
↓ activation	Bilateral SMA / cingulate	2575	0.0002	0,6,58	-4.577	~0	Left SMA BA 6, 32	762
							Right SMA BA 6, 32	648
							Left median cingulate BA 24, 32	457
							Right median cingulated BA 24, 32	430
							Left superior frontal gyrus BA 32	23
							Right superior frontal gyrus BA 6	70
							Left cingulum	56
							Right cingulum	23
							Left anterior cingulate BA 24	51
							Right anterior cingulate BA 24	19
	Right inf. frontal / insula	685	n.s.	52,14,-2	-4.102	~0	Right inferior frontal gyrus BA 48, 45	231
							Right insula BA 48, 47	181
							Right rolandic operculum BA 48	129
							Right superior temporal gyrus BA 38, 48	99
	Left precentral	414	n.s.	-40,-2,48	-3.783	~0	Left precentralgyrus BA 6	387
							Left postcentralgyrus BA 6	16

							Left middle frontal gyrus BA 6	11
	Left superior temporal	439	n.s.	-54,8,4	-3.758	~0	Left superior temporal gyrus BA 48, 38	165
							Left rolandic operculum, BA 48	162
							Left inferior frontal gyrus BA 48, 6	81
							Left insula BA 48	26
	Right temporal	144	n.s.	52,-40,12	-3.300	0.000002	Right superior temporal gyrus BA 42	72
							Right middle temporal gyrus BA 22	72
	Left precuneus	245	n.s.	-4,-50,54	-3.242	0.000003	Left precuneus BA 5	117
							Left median cingulate / paracingulategyri	57
							Right precuneus BA 5	63
	Right cuneus	99	n.s.	12,-72,38	-3.239	0.000003	Right cuneus cortex BA 7, 19	60
							Right precuneus BA 7	39
	Left precuneus	49	n.s.	-10,-74,38	-3.197	0.000004	Left precuneus BA 7	27
							Left cuneus cortex	13
	Left cerebellum	91	n.s.	-34,-60,-28	-3.128	0.000007	Left cerebellum	91
	Right putamen	38	n.s.	18,8,-10	-3.020	0.00002	Right putamen	11
	Left supramarginal	87	n.s.	-58,-26,24	-2.976	0.00003	Left supramarginalgyrus BA 48, 42	69
							Left superior temporal gyrus	12
	Right superior frontal	106	n.s.	0,32,-10	-2.882	0.00005	Right anterior cingulate BA 11	39
							Right superior frontal gyrus BA 11	26
							Left superior frontal gyrus BA 11	22
							Left anterior cingulated BA 11	19
	Right thalamus	26	n.s.	6,-14,6	-2.760	0.0001	Right thalamus	25
	Left superior parietal	22	n.s.	-18,-48,60	-2.716	0.0002	(undefined)	
	Cerebellum	11	n.s.	2,-64,-10	-2.675	0.0002	Vermis	10
Number of CS trials during conditioning								
↑ activation when many	Left basal ganglia	198	0.033	-6,4,4	3.819	0.00001	Left caudate nucleus	72
Reinforcement rate								
↓ activation with high	Right supramarginal	74	n.s.	52,-32,24	-2.993	0.00003	Right supramarginalgyrus BA 48	51
							Right superior temporal gyrus	10
↓ activation with high	Right insula	12	n.s.	28,28,-4	-2.675	0.0001	(undefined)	
Average CS–US delay								
↓ activation in delayed	Right supramarginal	67	n.s.	48,-32,24	-3.970	0.000006	Right supramarginalgyrus BA 48	42
↓ activation in delayed	Right precentral	38	n.s.	50,8,48	-3.526	0.00004	Right precentralgyrus BA 6	27
Use of electrical stimulation								
↑ activation with stimulation	Left supplementary motor area	137	n.s.	-10,-2,48	3.337	0.000002	Left supplementary motor area BA 6	47
				6,-2,50	2.777	0.00006	Right supplementary motor area	24
							Left median cingulate BA 24	66

							Right middle frontal gyrus	11
Use of a cognitive task								
↓ activation with task	Right insula	15	n.s.	44,8,-6	-2.485	0.0001	Right insula BA 48	15
↓ activation with task	Left insula	11	n.s.	-42,4,-8	-2.462	0.0002	Left insula	<10

Clusters with the main peak not overlapping any finding of the main analysis have been removed.
Only one local peak per gray matter brain region is displayed.
Only the two BA with more voxels are displayed

Abbreviations: GRF: Gaussian Random Field
Note: Cluster p-values refer to the GRF probability of finding clusters to that size according to the thresholds derived from the permutation test; when the maps were thresholded using threshold usual for GRF, many of the n.s. p-values became statistically significant.

Table 6S. Articles included in previous meta-analyses of fMRI human fear conditioning studies.

ETKIN & WAGER, 2007	Included in our meta-analysis?	Reason for exclusion
Armony & Dolan 2002[1]	No	No independent validation of conditioning
Buchel et al., 1998[2]	No	N<10
Buchel et al., 1999[3]	No	Trace conditioning
Chrichtley et al. 2002[4]	No	Not whole-brain fMRI
Gottfried & Dolan, 2004[5]	No	Not whole-brain fMRI
Gottfried et al., 2002[6]	No	Not whole-brain fMRI
Jensen et al., 2003[7]	No	Instructed fear
Knight et al., 2005[8]	No	No CS+ versus CS- comparison available
Phelps et al., 2004[9]	No	Instructed fear
Yaguez et al., 2005[10]	No	No independent validation of conditioning
MECHIAS ET AL., 2010		
Armony & Dolan, 2002[1]	No	No independent validation of conditioning
Birbaumer et al., 2005[11]	No	Not whole-brain fMRI
Buchel et al., 1998[2]	No	N<10
Buchel et al., 1999[3]	No	Trace conditioning
Chritchley et al., 2002[4]	No	Not whole-brain fMRI
Eippert et al., 2008[12]	Yes	
Gottfried et al., 2002[6]	No	Not whole-brain fMRI
Gottfried &Dolan, 2004[5]	No	Not whole-brain fMRI
Jensen et al., 2008[13]	No	No CS+ versus CS- comparison available
Kalisch et al., 2009[14]	Yes	
Knight et al., 2005[8]	No	No CS+ versus CS- comparison available
Schiller et al., 2008[15]	Yes	
Stark et al., 2006[16]	Yes	
Tabbert et al., 2005[17]	Yes	
Veit et al., 2002[18]	No	N<10

References

1. Armony JL, Dolan RJ. Modulation of spatial attention by fear-conditioned stimuli: an event-related fMRI study. *Neuropsychologia* 2002; **40:** 817-826.
2. Buchel C, Morris J, Dolan RJ, Friston KJ. Brain systems mediating aversive conditioning: an event-related fMRI study. *Neuron* 1998; **20:** 947-957.
3. Buchel C, Dolan RJ, Armony JL, Friston KJ. Amygdala-hippocampal involvement in human aversive trace conditioning revealed through event-related functional magnetic resonance imaging. *J Neurosci* 1999; **19:** 10869-10876.
4. Critchley HD, Mathias CJ, Dolan RJ. Fear conditioning in humans: the influence of awareness and autonomic arousal on functional neuroanatomy. *Neuron* 2002; **33:** 653-663.
5. Gottfried JA, Dolan RJ. Human orbitofrontal cortex mediates extinction learning while accessing conditioned representations of value. *Nature neurosci* 2004; **7:** 1144-1152.
6. Gottfried JA, O'Doherty J, Dolan RJ. Appetitive and aversive olfactory learning in humans studied using event-related functional magnetic resonance imaging. *J Neurosci*2002; **22:** 10829-10837.
7. Jensen J, McIntosh AR, Crawley AP, Mikulis DJ, Remington G, Kapur S. Direct activation of the ventral striatum in anticipation of aversive stimuli. *Neuron* 2003; **40:** 1251-1257.
8. Knight DC, Nguyen HT, Bandettini PA. The role of the human amygdala in the production of conditioned fear responses. *Neuroimage* 2005; **26:** 1193-1200.
9. Phelps EA, Delgado MR, Nearing KI, LeDoux JE. Extinction learning in

humans: role of the amygdala and vmPFC. *Neuron* 2004; **43:** 897-905.

10. Yaguez L, Coen S, Gregory LJ, Amaro E, Jr., Altman C, Brammer MJ *et al.* Brain response to visceral aversive conditioning: a functional magnetic resonance imaging study. *Gastroenterology* 2005; **128:** 1819-1829.
11. Birbaumer N, Veit R, Lotze M, Erb M, Hermann C, Grodd W *et al.* Deficient fear conditioning in psychopathy: a functional magnetic resonance imaging study. *ArchGen Psychiatry* 2005; **62:** 799-805.
12. Eippert F, Bingel U, Schoell E, Yacubian J, Buchel C. Blockade of endogenous opioid neurotransmission enhances acquisition of conditioned fear in humans. *J Neurosci*2008; **28:** 5465-5472.
13. Jensen J, Willeit M, Zipursky RB, Savina I, Smith AJ, Menon M *et al.* The formation of abnormal associations in schizophrenia: neural and behavioral evidence. *Neuropsychopharmacology* 2008; **33:** 473-479.
14. Kalisch R, Holt B, Petrovic P, De Martino B, Kloppel S, Buchel C *et al.* The NMDA agonist D-cycloserine facilitates fear memory consolidation in humans. *Cerebral Cortex* 2009; **19:** 187-196.
15. Schiller D, Levy I, Niv Y, LeDoux JE, Phelps EA. From fear to safety and back: reversal of fear in the human brain. *J Neurosci*2008; **28:** 11517-11525.
16. Stark R, Wolf OT, Tabbert K, Kagerer S, Zimmermann M, Kirsch P *et al.* Influence of the stress hormone cortisol on fear conditioning in humans: evidence for sex differences in the response of the prefrontal cortex. *Neuroimage* 2006; **32:** 1290-1298.
17. Tabbert K, Stark R, Kirsch P, Vaitl D. Hemodynamic responses of the amygdala, the orbitofrontal cortex and the visual cortex during a fear conditioning paradigm. *Int J Psychophysiol* 2005; **57:** 15-23.

18. Veit R, Flor H, Erb M, Hermann C, Lotze M, Grodd W *et al.* Brain circuits involved in emotional learning in antisocial behavior and social phobia in humans. *NeurosciLett* 2002; **328:** 233-236.

NEURAL SIGNATURES OF HUMAN FEAR CONDITIONING: AN UPDATED AND EXTENDED META-ANALYSIS OF FMRI STUDIES

Fullana et al.

SUPPLEMENTARY MATERIAL
Methods, Results, and Discussion

METHODS

Meta-analytic approach

Functional activation differences between the CS+ and the CS- were meta-analyzed using Anisotropic Effect-Size Signed Differential Mapping (AES-SDM) software, version 4.13 (www.sdmproject.com). [1, 2] AES-SDM is a novel neuroimaging meta-analytic approach that is capable of combining tabulated brain activation/deactivation results (i.e., regional peak statistic and coordinate information) with actual empirical voxel-wise "brain maps" of activations and deactivations (e.g., statistical parametric maps; SPMs) and which improves upon the positive features from existing peak probability methods for meta-analysis, such as Activation Likelihood Estimation (ALE)[3] or Multilevel Kernel Density Analysis (MKDA).[4]

Briefly, the method comprises three major steps. Firstly, whole brain maps of the effect size of the difference between the two conditions (CS+ and CS-) are recreated separately for each study, either from SPM or from the reported peak regional coordinate statistics. Secondly, these individual maps are meta-analyzed using well-established random-effects techniques of standard meta-analyses; these models are independently fitted in each voxel, but the statistical significance is derived from a whole-brain permutation test. Thirdly, a set of standard complementary analyses is conducted to further assess the robustness of the main findings.

Recreation of effect size maps when SPMs were available

Recreation of effect size maps from SPMs maps is straightforward as it only involves the transformation to Montreal Neurological Institute (MNI) stereotaxic space (in case that they were not already reported in this space) and the voxelwise conversion of t-

values (or alternatively p- or z-values) into effect sizes. Location of the maximum and minimum activity peaks in the recreated maps was manually checked to identify potential artifacts (e.g. image flip) during the conversion.

Recreation of effect size maps when only peak information was available

Recreation of effect size maps from peak information is more intensive. Specifically, effect-sizes are calculated following standard methods in those voxels containing a peak reported in the results table of the original studies, and for the remaining voxels, an effect-size is estimated depending on the distance to close peaks by means of an anisotropic unnormalized Gaussian kernel. This kernel assigns higher effect-sizes to those voxels more correlated with the peak, whereas small effect-sizes are assigned to those that, even if still neighboring, show only a small correlation at the population level. Both activations and deactivations are represented in the same map in order to correctly analyze those regions with higher between-study heterogeneity i.e., where some studies report activations and other deactivations. Note also that if activations and deactivations were plotted in separate maps, some brain regions may falsely appear as activating and deactivating at the same time in the same study – which is logically impossible.

To achieve a better recreation of the maps, we first derived the optimal parameters of the kernel (anisotropy and FWHM) with the following steps: 1) recreation of the effect size maps using only the peak statistics and coordinates of the 13 studies from which we obtained SPMs; 2) calculation of the mean square error between the effect size maps recreated using only the peak information and the effect size maps recreated using the SPMs; 3) repetition of steps *a* and *b* with different levels

of anisotropy and widths of the kernel to find the parameters with minimum mean square error. Best recreations of the 13 available SPMs from peak coordinates and t-values were achieved using a FWHM=20mm moderately (20-60%) anisotropic kernel, while poorer recreations were obtained when using kernels with FWHM <15mm or >35mm and no anisotropy. These parameters were thus used to recreate the effect size maps of the studies for which SPMs were not available.

RESULTS

Robustness analysis

Highly similar results were obtained when including only those studies reporting both activations and deactivations together (either within actual SPMs or from tabulated results), or when the meta-analysis was restricted to studies providing SPMs (all maps available upon request). Jackknife sensitivity analyses confirmed that results from the meta-analysis were highly replicable. All results corresponding to regional brain activations were preserved throughout the combination of all 27 datasets. Similarly, results were mostly identical when the meta-analysis was limited to studies considering negative peaks or when limited to studies from which we obtained SPMs. Finally, there was neither substantial heterogeneity, nor evidence of potential publication bias in the main activation and deactivation results (see **Table 2S**).

DISCUSSION

Meta-regression analyses

Our meta-regression results concur with the idea that some previous inconsistencies in the literature may have a methodological origin. [5] However, they should be interpreted cautiously given the low variability existing for some variables and/or the relatively low number of studies available for some of the comparisons. Furthermore, these analyses do not take into account the fact that different task-specific parameters are likely to interact at the brain-behavioral level[1]. Despite these caveats, most results are generally consistent with interpretations of the primary findings (see main manuscript) and other individual fear conditioning studies.

Younger age was associated with increased activation of commonly engaged regions during fear conditioning, including the right AIC. This result is in general agreement with previous accounts of the linear effects of age on autonomic reactivity [6] and with recent accounts of the importance of developmental aspects in fear learning. [7] With respect to task-specific features, we observed that the use of a pre-conditioning phase reduced activation of most components of the primary fear conditioning response, which seems analogous to the "latent inhibition" effect, i.e., where prior exposure to the CS decreases the rate of behavioral conditioning during later CS-US pairings. Although some learning theories do not account for this basic phenomenon,[8] others maintain that the CS-alone trials establish a context-CS association that primes the CS memory and thereby reduces its novelty/surprise during later CS-US pairings.[9] There have been very few direct demonstrations of the latent inhibition effect in human fear conditioning (see [10]) and its neural underpinnings remain poorly

[1] For example, as acknowledged in the primary text, the analysis of potential "US confounding" analyses was inherently limited by the fact that studies with such confounding were also generally the studies with higher reinforcement rates (because the former can only be analyzed by including reinforced trials).

understood. This meta-analysis suggests that fMRI can be used to study the neural processes of latent inhibition in human fear conditioning, and thus should be a topic of future research. Contrasting CS responses with versus without pre-conditioning or conditioning in the same context versus a different context to pre-conditioning, provide an experimental basis for a more detailed analysis of this phenomenon.

From the meta-regression analyses, we also observed that presenting more CSs trials during conditioning was associated with greater activation of the ventral caudate and nucleus accumbens, regions widely thought to mediate aversive prediction error signaling. [11] According to temporal difference learning theories, the prediction error signal initially peaks at the moment of US delivery (a fully unexpected US), but gradually shifts to the CS as the occurrence of the US becomes better predicted. [12] As conditioning trials continue, the peak is expected to move towards the earliest parts of the CS, perhaps making it more strongly detectable in fMRI, as suggested by this meta-analysis. One strength of the temporal difference learning approach is that it can explain second-order conditioning, another phenomenon that is unexplained by more traditional theories of learning.[8] Briefly, a neutral stimulus that is consistently followed by an established CS will also acquire the conditional response (fear), even in the absence of direct US pairings. The shifted prediction error signal makes the CS capable of supporting this type of second-order conditioning. Again, second-order conditioning is understudied in human fear conditioning, but a fruitful approach could be to manipulate the number of first-order CS-US conditioning trials and use the size of the neural prediction error signal to predict the strength of second-order conditioning in later phases (see also [12]).

We observed that the strength of activation of the dACC/dmPFC – discussed in the main text as potentially supporting aspects of conscious fear processing - was

diminished with a higher reinforcement rate. This finding may be consistent with the idea that introducing complexity (e.g., decreasing the reinforcement rate) places greater demands on conscious processing in terms of threat anticipation and threat appraisal. This topic seems especially important given the role threat uncertainty has in current models of anxiety[13]. Future meta-analyses may be able to address this question by comparing studies with ~0% or ~100% reinforcing rates (where uncertainty is lowest) with studies using ~50% reinforcing rate (where uncertainty is highest), and assessing the influence of reinforcement rate (modeled as an inverted U function) on dACC/dmPFC activity. Unfortunately there were not enough available studies to be able to conduct this analysis here.

Of note, it has been previously shown that changes in brain activity related to changes in reinforcement rates do not occur linearly in all brain regions. [14] In a similar vein, increasing the delay between the CS and the US was associated with increased activation in the vmPFC. This finding is reminiscent of the greater involvement of the prefrontal cortex in trace (in comparison to delay) fear conditioning. It has been suggested that this greater prefrontal involvement may be generalized to situations that involve higher temporal or contextual complexity, including higher delays between the CS and US in delay conditioning.[15]

We also observed that the use of a tactile electric shock US was associated with greater activation of the left caudal dorsal ACC/ventral SMA in comparison to other US types. This result is consistent with studies on pain perception, which suggest that although several areas (e.g., ACC, somatosensory areas) are commonly activated by different types of painful stimuli, there also appear to be discrete sub-regional differences in the processing of different types of pain.[16] Finally, the concurrent use of cognitive tasks reduced the strength of activation of the bilateral mid AIC, which is in

agreement with the idea that concurrent cognitive performance may reduce aversive interoceptive awareness, as suggested in previous studies on pain. [17]

There are other variables that may affect fear conditioning whose effect we could not investigate because of the lack of variation, including the type of US or the type of CS. Of note, the typical human experiment is characterized by self-selected low-intensity USs as well as high predictability and controllability of the experimental situation (via informed consent). Evolutionary theories have recommended the use of fear-relevant CSs (e.g. pictures of snakes or angry faces) to overcome these ethical limitations and activate threat-related brain areas in humans, [18] but only four studies in our meta-analysis used such stimuli. Systematical examination of the effects of different types of CSs on human brain activation would be highly relevant to the development of translational models of fear conditioning.

Finally, it would be highly informative in future fMRI studies if the impact of task-specific features on fear conditioning were thoroughly assessed across other modalities/domains (autonomic, behavioral, subjective). To our knowledge, there has been no comparable meta-analysis of other fear conditioning measures. Thus, it is unclear whether the general robustness and consistency of fMRI findings in fear conditioning studies is superior, for example, compared to fear conditioning measured via electrodermal (skin conductance) autonomic changes.

References

1. Radua J, Mataix-Cols D, Phillips ML, El-Hage W, Kronhaus DM, Cardoner N *et al.* A new meta-analytic method for neuroimaging studies that combines reported peak coordinates and statistical parametric maps. *Eur Psychiatry* 2012; **27:** 605-611.
2. Radua J, Rubia K, Canales-Rodriguez EJ, Pomarol-Clotet E, Fusar-Poli P, Mataix-Cols D. Anisotropic kernels for coordinate-based meta-analyses of neuroimaging studies. *Front Psychiatry* 2014; **5:** 13.
3. Eickhoff SB, Laird AR, Grefkes C, Wang LE, Zilles K, Fox PT. Coordinate-based activation likelihood estimation meta-analysis of neuroimaging data: a random-effects approach based on empirical estimates of spatial uncertainty. *Hum Brain Mapp* 2009; **30:** 2907-2926.
4. Wager TD, Lindquist M, Kaplan L. Meta-analysis of functional neuroimaging data: current and future directions. *Soc Cogn Affect Neurosci* 2007; **2:** 150-158.
5. Sehlmeyer C, Schoning S, Zwitserlood P, Pfleiderer B, Kircher T, Arolt V *et al.* Human fear conditioning and extinction in neuroimaging: a systematic review. *PLoS One* 2009; **4:** e5865.
6. Smith DP, Hillman CH, Duley AR. Influences of age on emotional reactivity during picture processing. *J Gerontol B Psychol Sci Soc Sci* 2005; **60:** 49-56.
7. Pattwell SS, Duhoux S, Hartley CA, Johnson DC, Jing D, Elliott MD *et al.* Altered fear learning across development in both mouse and human. *Proc Natl Acad Sci U S A* 2012; **109:** 16318-16323.

8. Rescorla RA, Wagner AR. A theory of Pavlovian conditioning: variations in the effectiveness of reinforcement and non reinforcement. In: Black AH, Prokasky WF (eds). *Classical conditioning II: current research and theory*. Appleton-Century-Crofts: New York, 1972.

9. Wagner AR. SOP: A model of automatic memory processing in animal behavior. In: Spear NE, Miller RR (eds). *Information processing in animals: memory mechanisms*. Erlbaum: Hillsdale, NJ, 1981.

10. Vervliet B. Latent Inhibition Speeds up but Weakens the Extinction of Conditioned Fear in Humans. *Journal of Psychology and Psychotherapy* 2013; **S7:** 2161-0487.

11. Delgado MR, Li J, Schiller D, Phelps EA. The role of the striatum in aversive learning and aversive prediction errors. *Philos Trans R Soc Lond B Biol Sci* 2008; **363:** 3787-3800.

12. Seymour B, O'Doherty JP, Dayan P, Koltzenburg M, Jones AK, Dolan RJ *et al.* Temporal difference models describe higher-order learning in humans. *Nature* 2004; **429:** 664-667.

13. Grupe DW, Nitschke JB. Uncertainty and anticipation in anxiety: an integrated neurobiological and psychological perspective. *Nat Rev Neurosci* 2013; **14:** 488-501.

14. Dunsmoor JE, Bandettini PA, Knight DC. Impact of continuous versus intermittent CS-UCS pairing on human brain activation during Pavlovian fear conditioning. *Behav Neurosci* 2007; **121:** 635-642.

15. Gilmartin MR, Balderston NL, Helmstetter FJ. Prefrontal cortical regulation of fear learning. *Trends Neurosci* 2014; **37:** 455-464.

16. Apkarian AV, Bushnell MC, Treede RD, Zubieta JK. Human brain mechanisms of pain perception and regulation in health and disease. *Eur J Pain* 2005; **9:** 463-484.

17. Seminowicz DA, Davis KD. A re-examination of pain-cognition interactions: implications for neuroimaging. *Pain* 2007; **130:** 8-13.

18. Mineka S, Ohman A. Phobias and preparedness: the selective, automatic, and encapsulated nature of fear. *Biol Psychiatry* 2002; **52:** 927-937.